Inorganic Chemistry

Article

pubs.acs.org/IC

Design and Synthesis of Heteroleptic Cyclometalated Iridium(III) Complexes Containing Quinoline-Type Ligands that Exhibit Dual Phosphorescence

Sarvendra Kumar,[†] Yosuke Hisamatsu,[†] Yusuke Tamaki,[‡] Osamu Ishitani,[‡] and Shin Aoki*[,†,§]

[†]Faculty of Pharmaceutical Science and [§]Imaging Frontier Cancer, Research Institute for Science and Technology, Tokyo University of Science, 2641 Yamazaki, Noda, Chiba 278-8510, Japan

[‡]Department of Chemistry, Graduate School of Science and Engineering, Tokyo Institute of Technology, 2-12-1-NE-1 O-okayama, Meguro-Ku, Tokyo 152-8550, Japan

Supporting Information

ABSTRACT: The design and synthesis of some cyclometalated iridium(III) complexes containing quinoline-type ligands as ancillary ligands are reported. The emission spectra of Ir(III) complexes containing a quinolinolate (**6**, **8**, **10**) moiety exhibit a single emission peak at ca. 590 nm, resulting in a red colored emission. However, Ir(III) complexes containing 8-sulfonamidoquinoline ligands (**11**, **13**−**21**) exhibit two different emission peaks (dual emission) at ca. 500 nm and ca. 600 nm upon excitation at 366 nm, resulting in a red-colored emission for **11** and a pale yellow-colored emission for **14**−**18** at 298 K. Especially, a white emission was observed for **19** at 298 and 77 K in dimethyl sulfoxide. The mechanistic studies based on time-dependent density functional theory calculations and time-resolved emission spectroscopy suggest that this dual emission originates from two independent emission states.

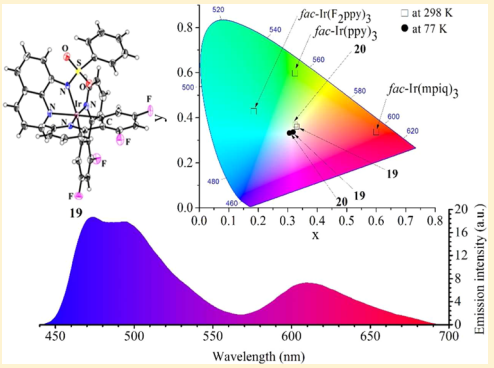

INTRODUCTION

Since the pioneering work of Forrest,[1] the design and synthesis of cyclometalated Ir(III) complexes such as **1** and **2** (Scheme 1) have received wide attention due to their high emission efficiency, excellent stability, and fact that the color emitted from them can be tuned from blue to red by varying the ligands.[2] These attractive photophysical properties of Ir(III) complex are now being applied to phosphorescent emitters for organic light-emitting diodes (OLEDs),[3] cell staining dyes,[4] pH sensors,[5] oxygen sensors,[6] molecules that induce and detect cell death,[7] and asymmetric photoredox catalysis.[8]

It is known that white OLEDs have been developed in all phosphor-doped devices with the potential for a 100% internal quantum efficiency.[9] In general, white light OLEDs require a combination of three different color emitters, blue, green and red, which is achieved by the deposition of multilayers on top of other components.[3b,10] Therefore, the development of metal complexes that exhibit a white emission (namely, a white emission from one compound) would be highly desirable in terms of reducing the fabrication cost and energy consumption of such materials.

The emission properties of cyclometalated Ir(III) complexes can generally be controlled by the cyclometalated ligands and/or ancillary ligands that are used. Recently, dual-emitting Ir(III) complexes have been reported to be attractive candidates for use as phosphorescent bioimaging probes.[11] For example, Lo and co-workers reported on a series of dual-emissive cyclometalated Ir(III) polypyridine complexes (**3a**−**d**) that function as luminescent sensors for various biomolecules (Scheme

Scheme 1

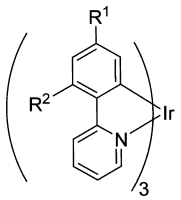

1a $(Ir(ppy)_3)$: $R^1 = R^2 = H$
1b $(Ir(tpy)_3)$: $R^1 = Me$, $R^2 = H$
1c $(Ir(mppy)_3)$: $R^1 = OMe$, $R^2 = H$
1d $(Ir(F_2ppy)_3)$: $R^1 = R^2 = F$

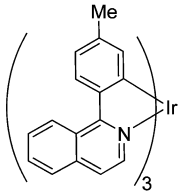

2 $(Ir(mpiq)_3)$

Received: December 11, 2015

DOI: 10.1021/acs.inorgchem.5b02872
Inorg. Chem. XXXX, XXX, XXX−XXX

2).[11c,g] In addition, Lippard and co-workers reported on a new class of dual-emissive cyclometalated Ir(III) complex **4** as a ratiometric sensor of Cu(II)[11d] and Zn(II).[11e]

Scheme 2

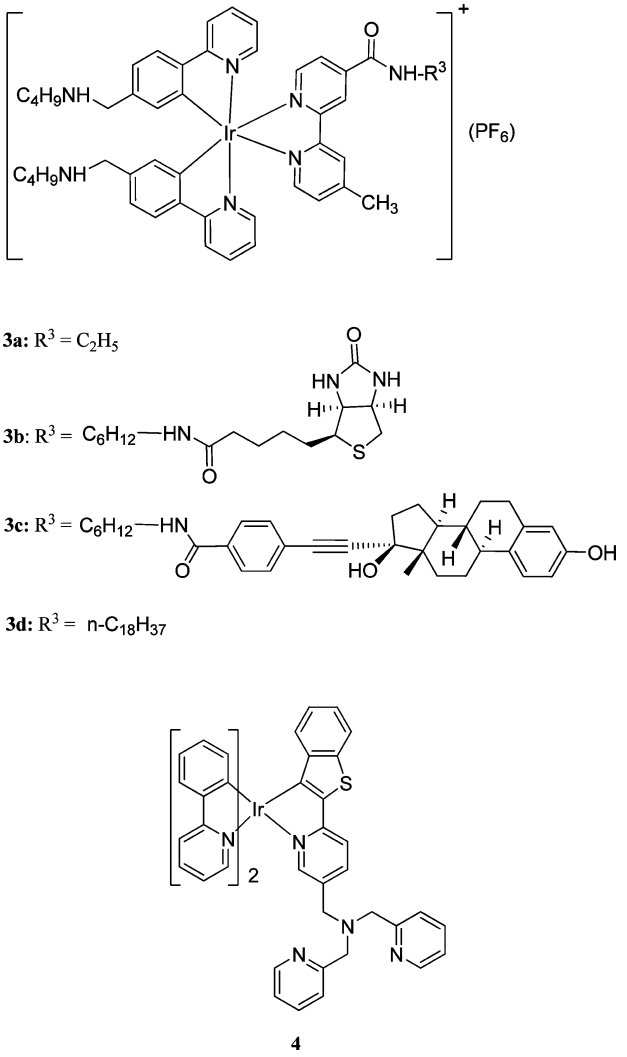

Meanwhile, quinoline derivatives have been reported to be versatile ligands for use in preparing luminescent complexes of aluminum(III) and other metals[12] as electroluminophores and electron-transporting compounds in OLEDs. For example, electronic $\pi-\pi^*$ transitions in the quinolinolate ligands of an AlQ_3 complex are responsible for light emission.[13] The highest occupied molecular orbital (HOMO) and lowest unoccupied molecular orbital (LUMO) of such complexes are located on the phenoxide moiety and the pyridyl side of the ligand, respectively,[14] and can affect the emission wavelength. To date, reports on the synthesis and photophysical properties of Ir(III)-quinolinolate complexes have appeared,[15] albeit their phosphorescence intensity is low ($\Phi < 0.01$) in solution.

Quinoline derivatives have also attracted considerable attention in several scientific fields,[16] and we have been involved in the research on the functions of 8-quinolinols as ligands in Zn^{2+}-selective fluorophores,[17a−c] potent inhibitors of dinuclear Zn^{2+} peptidase such as aminopeptidase from *Aeromonas proteolytica* (AAP),[17d−f] and potential candidates for radioprotective agents that can be used to reduce acute side effects of radiation therapy in the treatment of cancer.[17g,17h]

This background prompted us to synthesize a series of heteroleptic cyclometalated Ir(III) complexes containing quinoline-type ligands such as 8-quinolinols, 8-mercaptoquinoline, and 8-sulfonamidoquinoline as the ancillary ligand. We report herein on the design and synthesis of the Ir(III) complexes **5**−**8** and **10** with 8-quinolinol, **9** with 8-quinolinethiol, **12** with 8-aminoquinoline, and **11** and **13**−**21** with 8-sulfonamidoquinoline (Scheme 3), along with their crystal structures and photophysical properties. Among them, complexes **14**−**16** and **18**−**21** exhibit dual emission peaks at ca. 500 nm and ca. 600 nm at 298 K upon excitation at 366 nm in solution as well as in the solid state. The emission spectra of **11**, **14**, and **19** at low temperature (77 K) were also measured in glassy dimethyl sulfoxide (DMSO). It is noteworthy that compound **19**, which is composed of a cyclometalated 2-(2,4-difluorophenyl)pyridine (F_2ppy) ligand and an 8-sulfonamidoquinoline ligand, exhibits close to a white emission at both 298 and 77 K. Time-dependent density functional theory (TD-DFT) calculations were made, and time-resolved emission spectra were obtained to collect information on the possible mechanism for these phenomena.

RESULT AND DISCUSSION

Design and Synthesis of Ir(III) Complexes Having Quinoline Derivatives and Quinoline Sulfonamide. The Ir(III) complexes having quinolinol ligands (**5**−**8**) were prepared from dichloro-bridged dimeric complex **22** and 8-quinolinol (**23**) or the corresponding 8-hydroxyquinoline derivatives (**24**−**26**)[18] (Scheme 4). The complexes (**9**−**21**) were synthesized by the treatment of dichloro-bridged **22**,[19] **28**, **35**, and **36** with the ligands such as **24**, 8-quinolinethiol (**27**), 8-aminoquinoline (**29**), and the corresponding sulfonamidoquinoline derivatives (**30**−**34**).

Fine yellow crystals of **14**, **19**, and **20** were obtained by slow diffusion of hexanes to their solutions in $CHCl_3$ at room temperature. Their X-ray single-crystal structures are presented in Figure 1, and representative parameters and selected bond lengths are listed in Tables 1 and 2, respectively.

As shown in Figure 1, the two pyridines on ppy ligands of **14**, **19**, and **20** have a trans configuration, and bond lengths of Ir−N (ppy) and Ir−C (ppy) are 2.04−2.05 and 1.99−2.01 Å, respectively, which are consistent with those of $Ir(ppy)_2(acac)$ (acac: acetylacetonate).[20] In addition, the Ir−N (quinoline) and Ir−N (benzenesulfonamide) distances of **14**, **19**, and **20** are 2.13 and 2.18−2.19 Å. As shown in Figure 1a, the distance between the phenyl ring on the sulfonyl amide part and the centroid of the pyridine ring on the ppy ligand is 3.47 Å, which indicates face-to-face $\pi-\pi$ stacking interactions. However, such intramolecular interactions are minimal in the cases of **19** and **20** (Figure 1b,c).

Photophysical Properties of Heteroleptic Iridium Complexes. The UV−vis absoption spectra of **5**−**10** (10 μM) in DMSO at 298 K are presented in Figure 2. The absorption at ca. 275 nm is attributed to spin-allowed $\pi-\pi^*$ transitions of both the ppy ligands and the quinoline ligands. The complexes also exhibit a weak absorption in the region of ca. 350−500 nm, which is due to spin-allowed and spin-forbidden metal−ligand change transfer (MLCT) transitions and spin-forbidden $\pi-\pi^*$ transitions.[15,21] All of the compounds were recrystallized from $CHCl_3$ and hexanes at least twice before measurements of UV−vis absorption and emission

DOI: 10.1021/acs.inorgchem.5b02872
Inorg. Chem. XXXX, XXX, XXX−XXX

Scheme 3

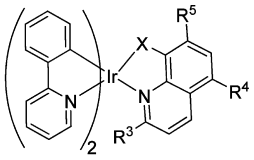

5: X = O, $R^3 = R^4 = R^5 = H$
6: X = O, R^3 = Me, $R^4 = R^5 = SO_2N(Me)_2$
7: X = O, R^3 = Me, $R^4 = SO_2N(Me)_2$, $R^5 = N(Me)_2$
8: X = O, R^3 = Me, $R^4 = R^5 = SO_2NHMe$
9: X = S, $R^3 = R^4 = R^5 = H$

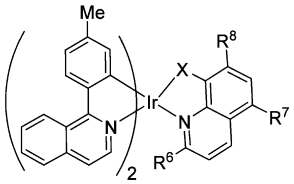

10: X = O, R^6 = Me, $R^7 = R^8 = SO_2N(Me)_2$
11: X = NSO_2Ph, $R^6 = R^7 = R^8 = H$

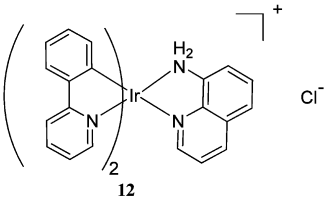

12

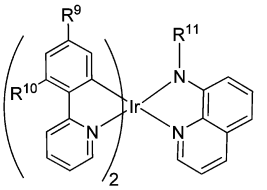

13: $R^9 = R^{10}$ = H, $R^{11} = SO_2Me$
14: $R^9 = R^{10}$ = H, $R^{11} = SO_2$–Ph
15: $R^9 = R^{10}$ = H, $R^{11} = SO_2$–Ph–Br
16: $R^9 = R^{10}$ = H, $R^{11} = SO_2$–Ph–OMe
17: $R^9 = R^{10}$ = H, $R^{11} = SO_2$–(quinolin-8-yl)
18: R^9 = OMe, R^{10} = H, $R^{11} = SO_2$–Ph
19: $R^9 = R^{10}$ = F, $R^{11} = SO_2$–Ph
20: $R^9 = R^{10}$ = F, $R^{11} = SO_2$–Ph–OMe
21: $R^9 = R^{10}$ = F, $R^{11} = SO_2Me$

spectra. Note also the exactly the same spectra were observed after recrystallization.

Emission spectra of **5**–**10** (10 μM) were measured in degassed DMSO at 298 K (excitation at 366 nm), and their quantum yields were determined based on the Φ value of $Ir(mpiq)_3$ (Φ = 0.26) used as a reference.[22] Although Ir(III) complexes **5**,[15b] **7**, and **9** exhibited very weak emissions at room temperature, **6**, **8**, and **10**, which contain sulfonylamide groups on the 5 and 7 positions of the quinoline ring, exhibit a red-colored emission at ca. 590–600 nm with Φ values of 0.13, 0.11, and 0.21, respectively, as shown in Figure 3. The emission lifetimes of the Ir(III) complexes **6**, **8**, and **10** are on a microsecond time scale, indicating that their emissions are due to excited triplet states. All of the photophysical data of **5**–**10** are summarized in Table 3.

We synthesized Ir(III) complexes **11** and **13**–**21**, containing 8-sulfonamidoquinoline ligands as the ancillary ligands. Their UV–vis absorption spectra in DMSO (10 μM) are shown in Figure S1 in Supporting Information. The absorption at ca. 275 nm is attributed to the spin-allowed π–π^* transitions of the phenylpyridyl and quinoline ligands. The complexes also exhibited a weak absorption in the region of ca. 350–530 nm, which are due to spin-allowed and spin-forbidden metal–ligand change transfer (MLCT) transitions and spin-forbidden π–π^* transitions. The excitation spectra of **11**, **14**, and **19** (10 μM), which were measured in degassed DMSO (Figure S2 in Supporting Information), were almost identical to their UV–vis absorption spectra. Photophysical data of **11**–**21** are summarized in Table 4.

The emission spectra of **11**–**21** in degassed DMSO (excitation at 366 nm) were measured at 298 K (Figure 4 and Table 4). Interestingly, it was found that **14**–**16** that contain arylsulfonamide groups (10 μM) exhibit dual emissions at ca. 500 nm (high energy (HE) emission band) and ca. 620 nm (low energy (LE) emission band; total $\Phi = 2.7 \times 10^{-2}$ for **14**, 3.7×10^{-2} for **15**, and 3.0×10^{-2} for **16**; Figure 4b). However, **13**, with a methylsulfonamide group, exhibits a broad emission (450 to 600 nm), but the intensity of the LEB is very weak as compared to the HEB (Figure 4a). Emission of **17** is very weak and is not included in Figure 4.

Ir(III) complexes **11** containing 1-(4-methylphenyl)-isoquinoline (mpiq), **18** containing 2-(4-methoxyphenyl)-pyridine (mppy), or **19**–**21** containing 2-(2,4-difluorophenyl)-pyridine (F_2ppy) were also prepared, because *fac*-$Ir(mpiq)_3$ (**4f**),[5d] *fac*-$Ir(mppy)_3$ (**4b**),[2c] and *fac*-$Ir(F_2ppy)_3$[11b] exhibit emissions at ca. 600 nm, ca. 497 nm, and ca. 475 nm, respectively. As shown in Figure 4c, the LEB for **18**–**21** is observed at ca. 620 nm. The HEB of **18** is observed at 487 and 512 nm, and those of **19**–**21** are observed as two emissions, possibly due to their vibrationally structured feature (**19**: 474, 493 nm, **20**: 476, 493 nm, and **21**: 478, 494 nm, respectively).

The emission spectrum of **12** having no sulfonamide group in degassed DMSO exhibits a broad emission band between 450 and 600 nm, suggesting that the presence of sulfonyl group at 8-amino group of **14**–**16** and **18**–**21** is essential for apparent dual color emission. The HEB of **14** and **19** were compared with *fac*- and *mer*-forms of $Ir(ppy)_3$ **1a** and $Ir(F_2ppy)_3$ **1d** (Figure S3 in Supporting Information). The fact that HEB of **14** and **19** are different from emission maxima of **1a** and **1d** indicates the contamination of **1a** and **1d** in the samples is highly unlikely.

The emission maxima of **14** in $CHCl_3$, CH_2Cl_2, DMSO, and toluene are summarized in Figure S4 in Supporting Information and Table 5, indicating that the peak height ratios between HEB and LEB are almost identical in different solvents.[23]

The emission spectra of **11**, **14**, and **19** in glassy DMSO[24] at 77 K exhibit a dual color emission with a hypsochromic shift due to the rigidochromic effect (Figure 5).[25] Note that **19** exhibits a white-color emission, possibly due to a hypsochromic shift.[24]

DOI: 10.1021/acs.inorgchem.5b02872
Inorg. Chem. XXXX, XXX, XXX–XXX

Scheme 4

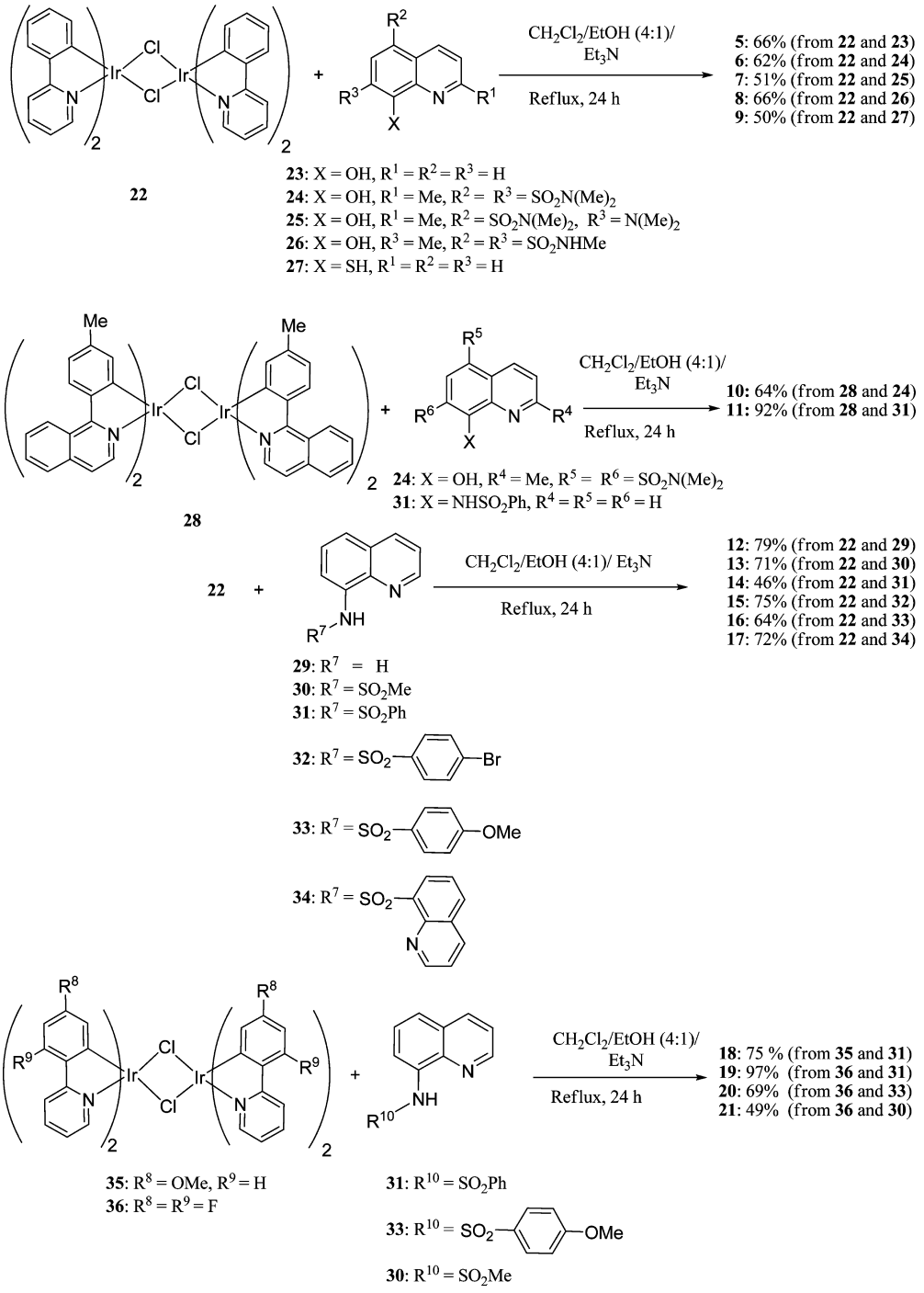

In the emission spectra of **13**–**17** at 298 K in the solid state, dual emission peaks (Figure S6 in Supporting Information) were observed, and the LE bands have a strong emission intensity compared to that in solutions. It should be added that **17** exhibits two peaks at 521 and 625 nm in the solid state, while its emission is very weak in solution.

In addition, the emission spectra of **11**, **14**, and **19** in 5 wt % doped in a poly(methyl methacrylate) (PMMA) polymer film (5 wt %) were measured at ambient temperature (samples of the PMMA film were prepared by using solutions of Ir(III) complexes and maintaining the films at 40 °C for 24 h). In the PMMA film, **11**, **14**, and **19** exhibited dual emission peaks with different peak ratios compared to those in solution (Figure S7 in Supporting Information), possibly due to the suppression of nonradiative pathways in the polymer.

Bunz and co-workers reported on the conversion of pictures colors to digital data.[26] In this work, we attempted a rather easy and convenient method. Namely, emission pictures of **11**, **14**, **19**, and **20** in degassed DMSO solutions were taken by several digital cameras. Then, we selected the appropriate cameras that exhibit similar colors as those recognized by our naked eyes and analyzed these pictures by using the Adobe Photoshop software without correction. In these measurements, we used at least 10 different points (10 different pixels) in the same picture and

DOI: 10.1021/acs.inorgchem.5b02872
Inorg. Chem. XXXX, XXX, XXX−XXX

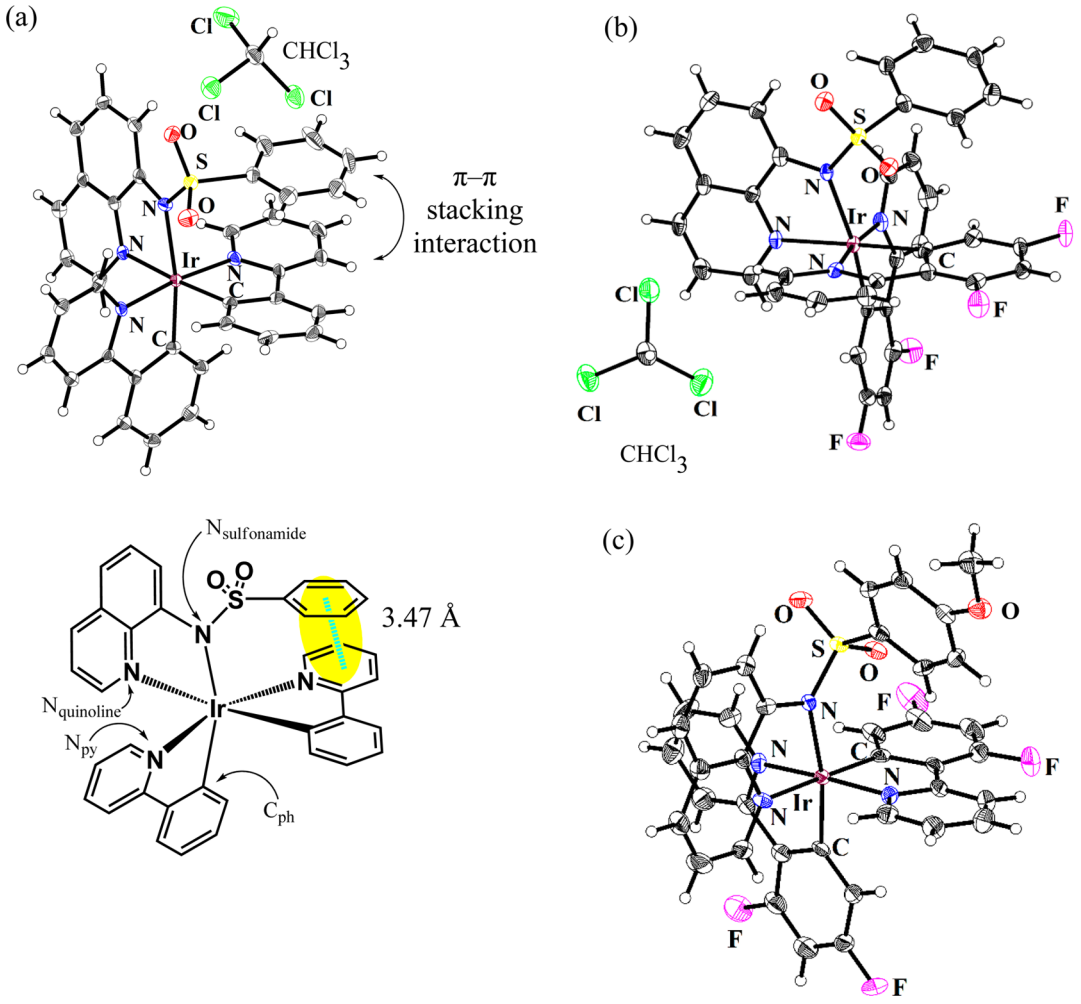

Figure 1. Perspective views of single crystal structures of (a) **14**, (b) **19**, and (c) **20** with 50% probability ellipsoids.

Table 1. Representative Crystallographic Parameters[a] of 14, 19, and 20

	14	19	20
empirical formula	$C_{37}H_{27}IrN_4O_2S{\cdot}CHCl_3$	$C_{37}H_{23}F_4IrN_4O_2S{\cdot}CHCl_3$	$C_{38}H_{25}F_4IrN_4O_3S$
M_r	903.27	975.22	885.88
crystal system	monoclinic	triclinic	triclinic
space group	$P21/n$	$P\bar{1}$	$P\bar{1}$
a (Å)	19.194(5)	11.477(5)	10.355(5)
b (Å)	9.114(5)	13.075(5)	11.129(5)
c (Å)	19.709(2)	13.777(5)	16.199(5)
α (deg)	90	73.813(5)	85.020(5)
β (deg)	101.926(5)	71.921(5)	77.980(5)
γ (deg)	90	66.201(5)	84.218(5)
V (Å^3)	3374(2)	1770.0(12)	1812.4(13)
Z	4	2	2
ρ_{calc} (g·cm^{-3})	1.778	1.830	1.623
R	0.028	0.0435	0.0336
R_w	0.0656	0.1096	0.0826
reflection measured/independent	17 488/6166	10 243/7103	9253/6502
observed ref [$I > 2\sigma(I)$]	5349	6326	5874
GOF	0.996	1.038	1.042

[a]The structures were solved by direct methods (Bruker APEX CCD) and refined by using least-squares techniques (SHELXL-97).

calculated average values to obtain RGB values of each sample. These RGB values were converted into *xy* color coordinates to be plotted in a chromaticity diagram (CIE 1931) as shown in Figure 6, by using the "Data-E calculator of the ColorMine library" (Table S1 in Supporting Information).[27] As displayed in Figure 6, **19** and **20** exhibit *xy* color coordinates (0.31, 0.32)

DOI: 10.1021/acs.inorgchem.5b02872
Inorg. Chem. XXXX, XXX, XXX−XXX

Table 2. Selected Bond Lengths (Å) of 14, 19, and 20

	14	19	20
Ir−N_{py}	2.04, 2.05	2.04, 2.04	2.04, 2.05
Ir−C_{ph}	2.00, 2.01	1.99, 2.00	1.99, 2.00
Ir−$N_{quinoline}$	2.13	2.13	2.13
Ir−$N_{sulfonamide}$	2.19	2.18	2.18

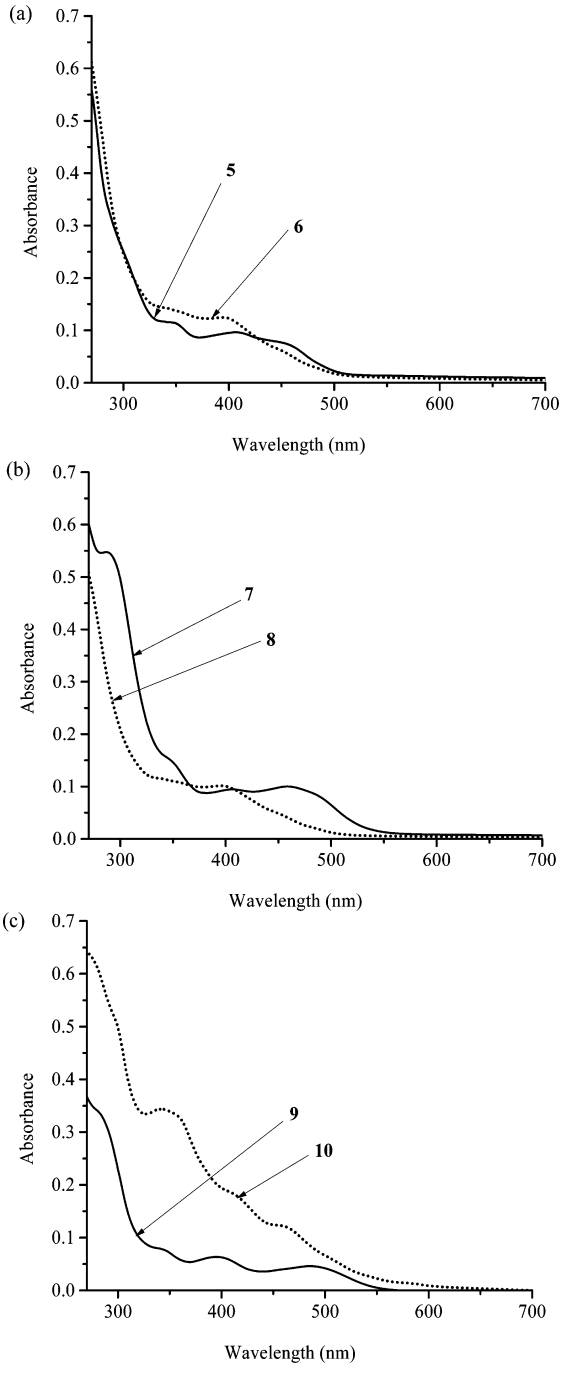

Figure 2. UV−vis spectra of Ir(III) complexes (a) **5** (plain curve), **6** (dotted curve), (b) **7** (plain curve), **8** (dotted curve), (c) **9** (plain curve), and **10** (dotted curve) in DMSO at 298 K ([Ir complex] = 10 μM).

corresponding to a white emission at 77 K, which are similar to those of white OLED (WOLED). For reference, a 2:5 mixture of **37**[2c] and **2** has *xy* color coordinates at $x = 0.31$ and $y = 0.33$

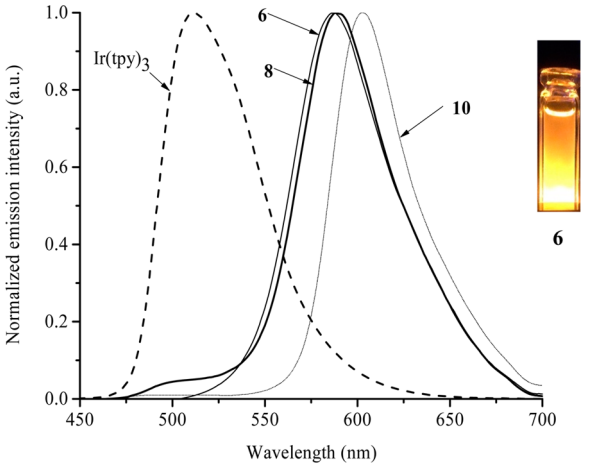

Figure 3. Normalized emission spectra of Ir(tpy)$_3$ (dashed curve), **6** (plain curve), **8** (bold curve), and **10** (short dotted curve) (10 μM) in degassed DMSO at 298 K ([Ir complex] = 10 μM and excitation at 366 nm). (inset) Picture of **6** (10 μM) taken under UV light (365 nm).

Table 3. Photophysical Properties[a] of 5−10 (10μM) in Degassed DMSO at 298 K

compound	UV−visible absorption maxima (nm)	emission maxima (nm)	quantum yield (Φ)	lifetime[b] τ (μs)
Ir(tpy)$_3$	300, 367, 453	516	0.50[c]	
5	351, 406, 456			
6	347, 400, 454	587	0.13	2.5
7	289, 350, 404, 464			
8	352, 400, 456	588	0.11	5.7
9	346, 399, 490			
10	345, 398, 489	600	0.21	2.0

[a]Excitation at 366 nm. Quantum yields were determined using Ir(mpiq)$_3$ as a reference (Φ = 0.26).[22] [b]A 475 nm long wave pass filter was used. [c]The quantum yield of Ir(tpy)$_3$ was determined using quinine sulfate in 0.1 M H_2SO_4 (ϕ = 0.55).

in DMSO at 298 K, which also produces a white-like colored emission.

Mechanistic Studies of Dual Emissions. To study the mechanism for the dual emission from the aforementioned Ir(III) complexes, TD-DFT calculations were performed for **6**, **8**, **10**−**16**, and **18**−**21** by using the Gaussian09 program.[28] The results are summarized in Figure 7 and Table 6 with the main transition characters. The HOMOs and LUMOs of **6**, **11**, **12**, **14**, and **19** are shown in Figure 7. In the case of **6**, the TD-DFT calculation results indicate that the emission peak at ca. 587 nm originates from $^3ML_{quin}CT + {}^3L_{quin}C$ transitions.

The major contribution of the triplet transition of **11**, exhibiting a single emission at 602 nm, is possibly due to HOMO−1 → LUMO ($^3ML_{mpiq}CT$). Interestingly, the HOMO of **12**, which is the parent compound of **14**, is localized on the phenyl ring of ppy, and the LUMO is localized on quinoline, exhibiting a single emission at 557 nm with a low quantum yield ($\Phi = 1.5 \times 10^{-2}$).

The experimental results of emission of **14** at 496 nm and at 617 nm (Figure 4b and Table 4) are in good agreement with theoretical values calculated by using TD-DFT (emissions at 493 and 652 nm) as listed in Table 6. Namely, the HOMO of **14** is mainly localized on the Ir center, quinoline ring (quin), and nitrogen atom (n) of the sulfonamide group of quinoline,

DOI: 10.1021/acs.inorgchem.5b02872
Inorg. Chem. XXXX, XXX, XXX−XXX

Table 4. Photophysical Properties of 11−21 (10 μM) in Degassed DMSO at 298 K (excitation at 366 nm)

		emission peaks (nm)			lifetime τ (μs)	
compounds	UV−vis absorption maxima (nm)	HEB[a]	LEB[a]	quantum yield[b] (Φ) HEB LEB (total)	HEB[c]	LEB[d]
11	294, 342, 445		602	0.35		3.25
12	347, 394, 424	557		1.5×10^{-2}		
13	343, 394, 444	500	623	0.12	1.63	
14	343, 393, 443	496	617	1.6×10^{-2} 1.1×10^{-2} (2.7×10^{-2})	4.26	8.95
15	341, 391, 441	496	611	3.2×10^{-2} 5.3×10^{-3} (3.7×10^{-2})	5.14	9.65
16	340, 394, 439	500	622	2.3×10^{-2} 7.4×10^{-3} (3.0×10^{-2})	2.98	7.88
17	346, 396, 446					
18	305, 374, 427	487, 512	617	3.6×10^{-2} 1.8×10^{-2} (5.4×10^{-2})	4.43	6.76
19	331, 366, 417	474, 493	613	8.3×10^{-2} 1.5×10^{-2} (9.8×10^{-2})	2.10	10.99
20	332, 370, 424	476, 493	617	4.5×10^{-2} 7.0×10^{-3} (5.2×10^{-2})	2.12	10.01
21	330, 367, 423	478, 494	615	4.8×10^{-2} 1.0×10^{-2} (5.8×10^{-2})	2.23	6.17

[a]HEB = higher energy emission band, and LEB = lower energy emission band. [b]Quantum yields for HEB and LEB were calculated and listed as well as total Φ values. [c]A 435 nm long wave pass filter was used. [d]A 550 nm long wave pass filter was used.

and its LUMO is localized on the quinoline ring, whereas LUMO+1 and LUMO+2 are mainly localized on the phenylpyridine (ppy) ligands (Figure 7). This suggests that the lowest-energy triplet excited state T_1 (1.90 eV), corresponding to an emission at 617 nm, is a mixture of $^3ML_{quin}CT$ (d(π) (Ir) → π*(quin)), $^3L_{quin}C$ (π(quin) → π*(quin)) and $^3IL_{quin}CT$ (n(sulfonamide) → π*(quin)) transitions. The second lowest-energy state T_2 (2.51 eV) of **14**, corresponding to an emission at 496 nm, is composed of $^3ML_{ppy}CT$ (d(π) (Ir) → π*(ppy)) and $^3L_{quin}L_{ppy}CT$ (π(quin) → π*(ppy)).

Similarly, lowest-energy triplet excited state T_1 (2.08 eV) for **19** is a mixture of $^3ML_{quin}CT$ (d(π) (Ir) → π*(quin)), $^3L_{quin}C$ (π(quin) → π*(quin)) and $^3IL_{quin}CT$ (n(sulfonamide) → π*(quin)) transitions (613 nm) by calculation, and its second lowest-energy state T_2 (2.76 eV) is composed of $^3ML_{F2ppy}CT$ (d(π) (Ir) → π*(F_2ppy)) and $^3L_{quin}L_{ppy}CT$ (π(quin) → π*(F_2ppy)) (476 nm by calculation). Then we conclude that these two main transition states, T_1 and T_2, contribute to the dual emission of Ir(III) complexes **14**−**21** (Scheme 5).

You et al. reported on tuning of the emission color of heteroleptic Ir(III) complexes consisting of F_2ppy ligands and a variety of ancillary ligands.[29] They concluded that the interligand energy transfer between the cyclometalated F_2ppy ligand and the corresponding ancillary ligand is the most probable mechanism, as supported by time-resolved emission spectroscopy and the observation that the rise component in time-resolved emission spectrum is strong evidence of an interligand energy transfer.[29b]

Therefore, we hypothesize that the interligand energy transfer ($T_1 \rightleftharpoons T_2$ in Scheme 5) from HEB to LEB can be attributed to dual emissions in our Ir(III) complexes, which prompted us to measure the emission decay of **14** and **19** (excitation at 371 nm) at both HEB and LEB by using time-resolved emission spectroscopy (Figure S8 in Supporting Information and Figure 8). The emission decay of **14** at 496 nm provided a single-component emission lifetime of 1.7 μs, and biexponential emission decay is observed at 617 nm (τ = 1.3 and 12 μs; Figure S8a in Supporting Information and Table 7; for comparison, the emission decay of **11** is shown in Figure S8b in Supporting Information). The biexponential emission decay at 617 nm (LEB) is deconvoluted into a prompt decay component (τ = 1.3 μs), whose contribution is 4% at 617 nm and a slower decay (τ = 12 μs), whose contribution is 96% at the same wavelengths (Table 7). The prompt decay of LEB (1.3 μs) possibly corresponds to tailing of HEB.

Similar results were obtained from the emission decay curves of **19**, which provide a single-component emission lifetime of 1.9 μs at 474 and 493 nm, respectively, and biexponential emission lifetimes of 1.8 and 17 μs at 613 nm (Figure 8 and Table 7). The time-resolved emission spectra indicate that both HEB and LEB have lifetimes of ca. 1−2 μs and that LEB becomes dominant with a delay time of up to ca. 6 μs. In both time-resolved emission spectra, observed rise components are negligible, and the emission maxima and lifetimes of HEB of **14** (τ = 1.7 μs) and **19** (τ = 1.9 μs) are nearly identical to those of $Ir(ppy)_2(acac)$ (τ = 1.6 μs)[20] and $Ir(F_2ppy)_2(acac)$ (τ = 1.0 μs).[30] These results suggest that interligand energy transfer between T_1 and T_2 is unlikely and that the dual emission of **14** and **19** originates from the two independent emission states, T_1 and T_2,[11,31] although we do not completely exclude the possibility of very slow energy transfer from T_2 to T_1.

CONCLUSION

In conclusion, we report herein on the synthesis and photophysical properties of heteroleptic cyclometalated iridium(III) complexes having the variety of quinoline derivatives as ancillary ligands. The findings indicate that **14**−**16** and **18**−**21** containing 8-sulfonamidoquinolines exhibit a dual color emission at ca. 500 nm and ca. 600 nm upon excitation at 366 nm at 298 K, and especially, **19** exhibits a white-color emission at 298 K and at 77 K, as displayed in chromaticity diagram (Figure 6) prepared by using digital camera and convenient data conversion. The presence of sulfonyl group on 8-aminoquinoline unit is essential for dual color emission. The results of theoretical (TD-DFT) calculations and time-resolved emission spectroscopy suggest that dual emission of these complexes originates from two independent emission states. This information provides useful information for the design and synthesis of new metal complexes and their applications to OLEDs and related materials.

EXPERIMENTAL SECTION

General Information. $IrCl_3 \cdot 3H_2O$ was purchased from Kanto Chemical Co. ^1H NMR spectra (300 MHz) was recorded on a JEOL Always 300 spectrometer. Electrospray ionization (ESI) mass spectra (MS) were recorded on a Varian 910-MS. Thin-layer (TLC) and silica gel column chromatographies were performed using Merck 5554

DOI: 10.1021/acs.inorgchem.5b02872
Inorg. Chem. XXXX, XXX, XXX−XXX

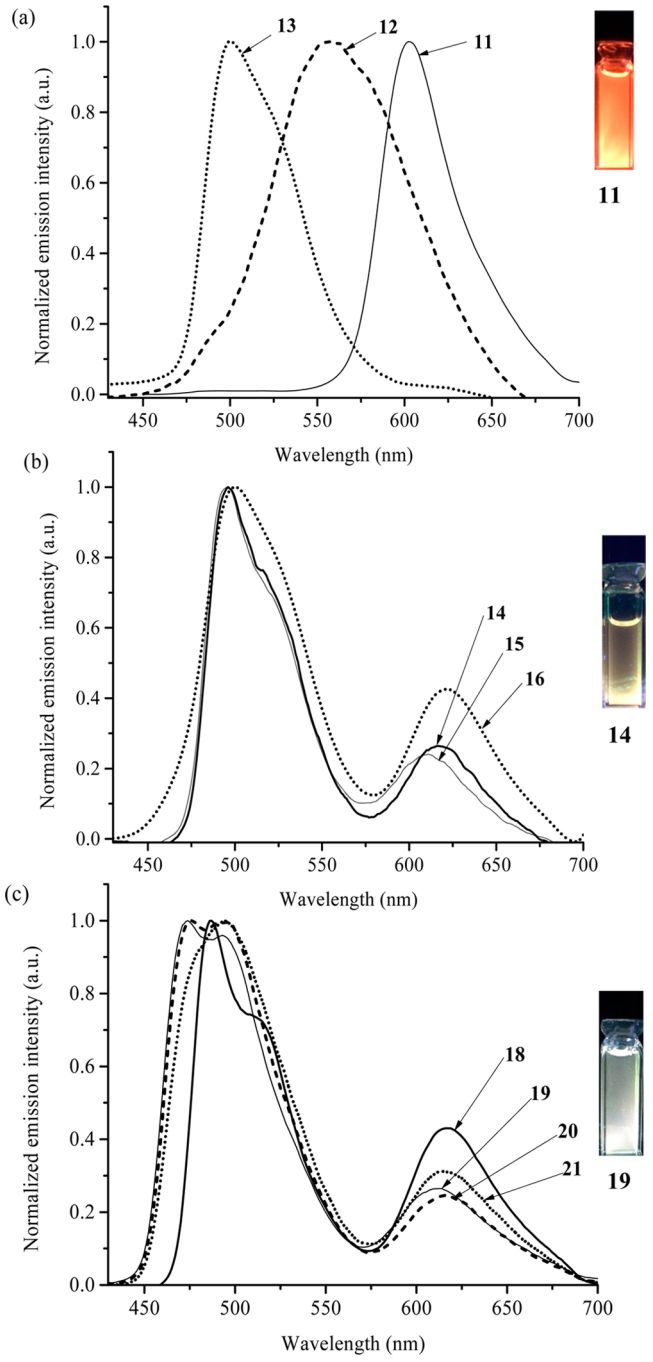

Figure 4. Normalized emission spectra of (a) **11** (plain curve), **12** (dashed curve), and **13** (dotted curve), (b) **14** (bold curve), **15** (plain curve), and **16** (short dotted curve), and (c) **18** (bold curve), **19** (plain curve), **20** (dashed curve), and **21** (short dotted curve) in degassed DMSO at 298 K ([Ir complex] = 10 μM and excitation at 366 nm). (inset) Pictures of **11**, **14**, and **19** (10 μM) taken under UV light (365 nm).

(silica gel) TLC plates and Fuji Silysia Chemical FL-100D, respectively. Emission lifetimes were determined using a TSP-1000 (Unisoku Co, Ltd). Density functional theory (DFT) calculations[28] were also carried out using the Gaussian09 program (B3LYP, the LanL2DZ basis set for a Ir atom and the 6-31G basis set for H, C, S, Br, O, N atoms). The commercial available DMSO (spectrophotometric grade, Wako Chemical Co) was used for the measurement of photophysical data. Negligible hazard exists in all synthetic procedures.

*Synthesis of Di-μ-chloro-tetrakis[k²(C2,N)-2-phenylpyridine]-diiridium(III) (**22**).* $IrCl_3 \cdot 3H_2O$ was suspended in a mixture of 2-ethoxyethanol and water under Ar, to which 2-phenylpyridine had been added. The resulting reaction mixture was stirred at 110 °C for 24 h to afford a dark brown reaction mixture containing a yellow precipitate. The precipitate was isolated on a filter, washed with water, ethanol, and acetone, and dried under vacuo. The NMR spectrum of the material was found to be identical with that reported in the literature.[19a]

Di-μ-chloro-tetrakis[k^2(C2,N)-2-mppy]diiridium(III) **35**[19b] and di-μ-chloro-tetrakis[k^2(C2,N)-2-dfppy]diiridium(III) **36**[19c] were synthesized in a similar manner and were used for preparing **22**.

Synthesis of Quinoline Derivatives. Compounds (**24**–**26**) were synthesized as described in our previous paper.[17g,18] The 8-sulfonamidoquinoline ligands (**29**–**34**) were synthesized by reacting 8-aminoquinoline with the corresponding sulfonyl chlorides in pyridine at 130 °C under microwave conditions.[32] Reaction mixtures were then poured into water, and the resulting solid was isolated on a filter and washed with water. When no precipitate was formed, the product was obtained by extracting the aqueous phase twice with CH_2Cl_2. The organic layer was then dried over anhydrous sodium sulfate and evaporated in vacuo to obtain a solid.

*N-(Quinolin-8-yl)methylsulfonamine (**30**).* Yield = 51% (40 mg). Brown color solid. mp 132 °C. IR (ATR): ν = 3287, 1504, 1472, 1305, 1146, 1087, 970, 829, 760, 545, 508 cm^{-1}. ^1H NMR (300 MHz, $CDCl_3$) δ 8.93 (s, 1H), 8.83 (d, J = 4.2 Hz, 1H), 8.20 (d, J = 8.3 Hz, 1H), 7.87 (d, J = 6.9 Hz, 1H), 7.54 (ddd, J = 12.5, 8.9, 5.4 Hz, 3H), 3.04 (s, 3H) ppm. EI-MS (m/z): Calcd for $C_{10}H_{10}N_2O_2S$ (M^+): 222.0453. Found: 222.0467.

Table 5. Emission Peaks of 14 (10 μM) in Various Solvents at 298 K, and 11, 14, and 19 at 77 K

		emission maxima (nm)		temperature
complex	solvent	HEB[a]	LEB[a]	(K)
14	DMSO	496	617	298
14	$CHCl_3$	491	613	298
14	CH_2Cl_2	491	611	298
14	toluene	496	623	298
14	DMSO	483, 516	581	77
11	DMSO		597	77
19	DMSO	457, 489	567	77

[a]Excitation at 366 nm. HEB = higher energy emission band, and LEB = lower energy emission band.

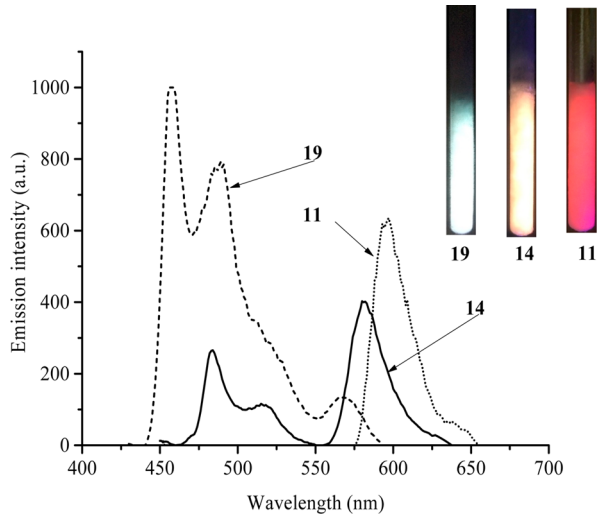

Figure 5. Emission spectra of **11** (short dotted curve), **14** (bold curve), and **19** (dashed curve) in glassy DMSO at 77 K. (inset) Emission pictures of **11**, **14**, and **19** in glassy DMSO ([Ir complex] = 10 μM and excitation at 366 nm).

DOI: 10.1021/acs.inorgchem.5b02872
Inorg. Chem. XXXX, XXX, XXX−XXX

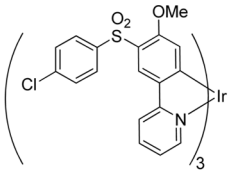

37

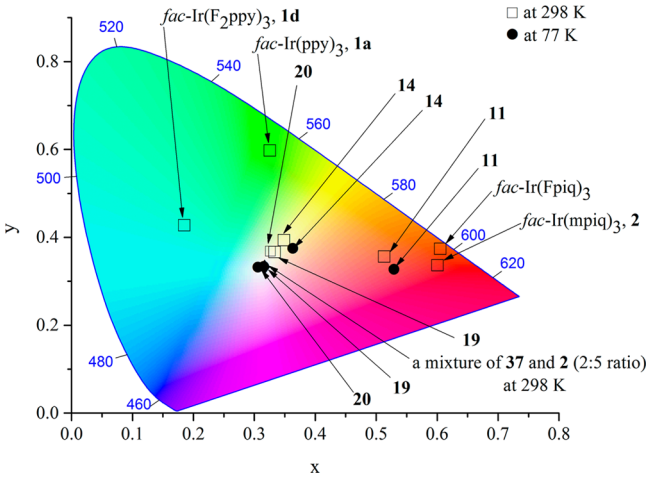

Figure 6. Chromaticity diagram showing the *xy* color coordinates of **11**, **14**, **19**, **20**, and **37**+**2** (CIE 1931). The *xy* color coordinates of these complexes were calculated from their RGB values. For details, see Table S1 in Supporting Information.

*N-(Quinolin-8-yl)benzenesulfonamine (**31**).* Yield = 57% (56 mg). Off-white color solid. mp 120 °C. IR (ATR): ν = 3215, 1503, 1407, 1355, 1306, 1160, 1086, 926, 785, 716, 684, 568, 557 cm^{-1}. ^1H NMR (300 MHz, $CDCl_3$) δ 9.25 (s, 1H), 8.76 (dd, J = 4.2, 1.7 Hz, 1H), 8.10 (dd, J = 8.3, 1.6 Hz, 1H), 7.97−7.87 (m, 2H), 7.84 (dd, J = 6.3, 2.7 Hz, 1H), 7.45 (dd, J = 3.9, 2.5 Hz, 3H), 7.43−7.35 (m, 3H) ppm. EI-MS (m/z): Calcd for $C_{10}H_{12}N_2O_2S$ (M^+): 284.0619. Found: 284.0616.

*4-Bromo-N-(quinolin-8-yl)benzenesulfonamine (**32**).* Yield = 49% (62 mg). Off-white color solid. mp 218 °C. IR (ATR): ν = 3223, 1572, 1504, 1410, 1268, 1304, 1157, 1084, 796, 740, 668, 614, 553 cm^{-1}. ^1H NMR (300 MHz, $CDCl_3$) δ 9.23 (s, 1H), 8.76 (s, 1H), 8.12 (d, J = 8.2 Hz, 1H), 7.83 (d, J = 7.1 Hz, 1H), 7.77 (d, J = 8.7 Hz, 2H), 7.52−7.42 (m, 5H) ppm. EI-MS (m/z): Calcd for: $C_{15}H_{11}BrN_2O_2S$ (M^+): 361.9725. Found: 361.9724.

*4-Methoxy-N-(quinolin-8-yl)benzenesulfonamine (**33**).* Yield = 73% (80 mg). Gray color solid. mp 75 °C. IR (ATR): ν = 3267, 1593, 1504, 1470, 1412, 1363, 1259, 1150, 1085, 920, 824, 787, 667, 549 cm^{-1}. ^1H NMR (300 MHz, $CDCl_3$) δ 9.20 (s, 1H), 8.76 (dd, J = 4.2, 1.7 Hz, 1H), 8.10 (dd, J = 8.3, 1.6 Hz, 1H), 7.91−7.75 (m, 3H), 7.53−7.34 (m, 3H), 6.92−6.70 (m, 2H), 3.76 (s, 3H) ppm. EI-MS (m/z): Calcd for $C_{16}H_{14}N_2O_3S$ (M^+): 314.0725. Found: 314.0727.

*N-(Quinolin-8-yl)quinoline-8-sulfonamine (**34**).* Yield = 59% (69 mg). White color solid. mp 232 °C. IR (ATR): ν = 3165, 1501, 1469, 1411, 1269, 1306, 1167, 1144, 834, 768, 700, 588, 502 cm^{-1}. ^1H NMR (300 MHz, $CDCl_3$) δ 10.55 (s, 1H), 9.20−9.00 (m, 1H), 8.75−8.57 (m, 1H), 8.52 (d, J = 7.3 Hz, 1H), 8.21−8.03 (m, 1H), 8.04−7.83 (m, 3H), 7.64−7.48 (m, 1H), 7.46 (dd, J = 8.3, 4.3 Hz, 1H), 7.41−7.28 (m, 3H) ppm. EI-MS (m/z): Calcd for $C_{18}H_{13}N_3O_2S$ (M^+): 335.0728. Found: 335.0722.

*Synthesis of Ir Complexes **5**−**21**.* A general method was used for preparing all of complexes: di-μ-chloro-tetrakis[$k^2(C_2,N)$-2-phenylpyridine]diiridium(III) **22** (1 equiv) was dissolved in a mixture of CH_2Cl_2 and EtOH (4:1 ratio), and the 8-hydroxyquinoline derivatives (2.2 equiv) and Et_3N (45 equiv) were then added. The reaction mixture was refluxed for 20 h under argon. After evaporation of the solvent, the residue was washed with ethanol to remove unreacted ligand, and the resulting product was purified by silica gel chromatography with $CHCl_3$ as an eluent and recrystallized from hexanes/$CHCl_3$ or hexanes/CH_2Cl_2. Similar procedure was used for the synthesis of Ir(III) complexes from dichloro-bridged Ir(III) complexes **28**, **35**, and **36** and quinoline derivatives.

5: Yield = 66% (16 mg). Yellow color solid. mp > 300 °C. IR (ATR): ν = 3370, 1603, 1567, 1457, 1384, 1324, 1221, 1157, 1058, 1028, 819, 728, 616, 508 cm^{-1}. ^1H NMR (300 MHz, $CDCl_3$) δ 8.81 (d, J = 4.7 Hz, 1H), 7.99 (d, J = 8.4 Hz, 1H), 7.87 (d, J = 7.9 Hz, 1H), 7.80 (d, J = 7.8 Hz, 1H), 7.67 (d, J = 6.2 Hz, 2H), 7.60 (d, J = 7.8 Hz, 4H), 7.54 (d, J = 5.8 Hz, 1H), 7.42 (t, J = 8.0 Hz, 1H), 7.10 (dd, J = 8.4, 4.8 Hz, 1H), 7.03 (m, 2H), 6.96−6.85 (m, 2H), 6.84−6.72 (m, 3H), 6.45 (d, J = 7.9 Hz, 1H), 6.30 (d, J = 6.9 Hz, 1H) ppm. ESI-MS (m/z): Calcd for $C_{31}H_{23}N_3O(^{191}Ir)$ ($M+H^+$): 644.1442. Found: 644.1443. Elemental analysis was not carried out because the content of iridium in **5** is >25%.

6: Yield = 62% (20 mg). Red color solid. mp > 300 °C. IR (ATR): ν = 1606, 1538, 1477, 1417, 1314, 1135, 1030, 961, 788, 716, 627, 552 cm^{-1}. ^1H NMR (300 MHz, $CDCl_3$) δ 8.89 (d, J = 8.8 Hz, 1H), 8.58 (d, J = 6.3 Hz, 1H), 8.49 (s, 1H), 7.89 (d, J = 8.4 Hz, 2H), 7.73 (t, J = 7.5 Hz, 2H), 7.63 (d, J = 8.0 Hz, 1H), 7.54 (d, J = 6.9 Hz, 2H), 7.33 (d, J = 8.8 Hz, 1H), 7.12 (s, 1H), 6.95−6.82 (m, 3H), 6.75 (d, J = 7.4 Hz, 2H), 6.39 (d, J = 6.7 Hz, 1H), 6.02 (d, J = 7.7 Hz, 1H), 2.84 (s, 6H), 2.24 (s, 6H), 2.14 (s, 3H) ppm. ESI-MS (m/z): Calcd for $C_{36}H_{34}N_5O_5S_2(^{191}Ir)$ (M^+): 871.1602. Found: 871.1604. Anal. Calcd for $C_{36}H_{34}IrN_5O_5S_2{\cdot}0.25CHCl_3$: C, 48.22; H, 3.82; N, 7.76. Found: C, 48.60, H, 4.02; N, 7.49%.

7: Yield = 51% (20 mg). Red color solid. mp > 300 °C. IR (ATR): ν = 1587, 1538, 1502, 1456, 1315, 1138, 1048, 962, 815, 788, 815, 788, 719, 676, 577, 554 cm^{-1}. ^1H NMR (300 MHz, $CDCl_3$) δ 8.94 (s, 2H), 8.86 (d, J = 8.8 Hz, 1H), 8.17 (d, J = 8.3 Hz, 1H), 8.00 (d, J = 8.1 Hz, 1H), 7.87 (s, 2H), 7.73 (dd, J = 7.7, 5.6 Hz, 4H), 7.45−7.34 (m, 2H), 7.31 (s, 1H), 7.18 (d, J = 6.2 Hz, 1H), 6.77 (s, 2H), 6.23 (s, 1H), 5.99 (s, 1H), 2.82 (s, 6H), 2.13 (s, 6H), 2.01 (d, J = 1.9 Hz, 3H) ppm. ESI-MS (m/z): Calcd for $C_{36}H_{34}N_5O_3S(^{191}Ir)$ (M^+): 807.1988. Found: 807.1985. Anal. Calcd for $C_{36}H_{34}IrN_5O_5S_2{\cdot}0.33CHCl_3$: C, 51.41; H, 4.08; N, 8.25. Found: C, 51.59, H, 4.00; N, 7.94%.

8: Yield = 66% (52 mg). Orange color solid. mp > 300 °C. IR (ATR): ν = 1606, 1582, 1535, 1476, 1417, 1313, 1145, 1060, 970, 831, 754, 729, 667, 553 cm^{-1}. ^1H NMR (300 MHz, $CDCl_3$) δ 8.92 (d, J = 8.8 Hz, 1H), 8.66−8.40 (m, 2H), 7.90 (dd, J = 8.0, 4.3 Hz, 2H), 7.79−7.68 (m, 2H), 7.65 (d, J = 7.8 Hz, 1H), 7.57 (d, J = 7.8 Hz, 1H), 7.43 (d, J = 5.7 Hz, 1H), 7.38 (d, J = 7.5 Hz, 1H), 7.10 (ddd, J = 7.3, 5.8, 1.4 Hz, 1H), 6.97−6.83 (m, 3H), 6.82−6.71 (m, 2H), 6.42−6.33 (m, 1H), 5.99 (d, J = 7.6 Hz, 1H), 5.23 (q, J = 5.5 Hz, 1H), 4.46 (d, J = 5.4 Hz, 1H), 2.72 (d, J = 5.4 Hz, 2H), 2.15 (d, J = 7.0 Hz, 4H), 1.87 (d, J = 5.5 Hz, 3H) ppm. ESI-MS (m/z): Calcd for $C_{34}H_{30}N_5O_5S_2(^{191}Ir)$ (M^+): 843.1288. Found: 843.1286. Anal. Calcd for $C_{34}H_{30}IrN_5O_5S_2{\cdot}0.33CHCl_3$: C, 46.61; H, 3.46; N, 7.92. Found: C, 46.40, H, 3.18; N, 7.66%.

9: Yield = 50% (17 mg). Red color solid. mp > 300 °C. IR (ATR): ν = 1604, 1553, 1474, 1415, 1335, 1294, 1267, 1208, 1159, 1060, 1028, 999, 820, 752, 681, 630, 560 cm^{-1}. ^1H NMR (300 MHz, $CDCl_3$) δ 9.80 (d, J = 6.5 Hz, 1H), 8.02 (t, J = 6.5 Hz, 2H), 7.89−7.80 (m, 3H), 7.70−7.54 (m, 4H), 7.39 (d, J = 5.7 Hz, 1H), 7.33 (d, 6.2 Hz, 2H), 7.14 (d, J = 8.0 Hz, 1H), 7.08 (d, J = 5.0 Hz, 1H), 7.00 (t, J = 7.2 Hz, 2H), 6.91 (d, J = 3.8 Hz, 1H), 6.83−6.73 (m, 2H), 6.47 (d, J = 7.2 Hz, 1H), 6.32 (d, J = 7.6 Hz, 1H) ppm. ESI-MS (m/z): Calcd for $C_{31}H_{22}N_3S$ (^{191}Ir) ($M+H^+$): 659.1134. Found: 659.1128. Elemental analysis was not carried out because the content of iridium in **9** is >25%.

10: Yield = 64% (16 mg). Red color solid. mp > 300 °C. IR (ATR): ν = 1605, 1582, 1512, 1475, 1446, 1415, 1323, 1263, 1208, 1136, 1060, 1030, 945, 808, 728, 639, 570 cm^{-1}. ^1H NMR (300 MHz, $CDCl_3$) δ 8.94 (s, 2H), 8.86 (d, J = 8.8 Hz, 1H), 8.49 (t, J = 3.2 Hz, 2H), 8.17 (d, J = 8.3 Hz, 1H), 8.00 (d, J = 8.1 Hz, 1H), 7.87 (s, 2H), 7.76−7.70 (m, 4H), 7.45−7.34 (m, 2H), 7.31 (s, 1H), 7.18 (d, J = 6.2 Hz, 1H), 6.77 (s, 2H), 6.23 (s, 1H), 5.99 (s, 1H), 2.82 (s, 6H), 2.13 (s, 9H), 2.03 (s, 3H), 2.01 (s, 3H) ppm. ESI-MS (m/z): Calcd for $C_{46}H_{42}N_5O_5S_2(^{191}Ir)$ (M^+): 999.2223. Found: 999.2208. Anal. Calcd

DOI: 10.1021/acs.inorgchem.5b02872
Inorg. Chem. XXXX, XXX, XXX−XXX

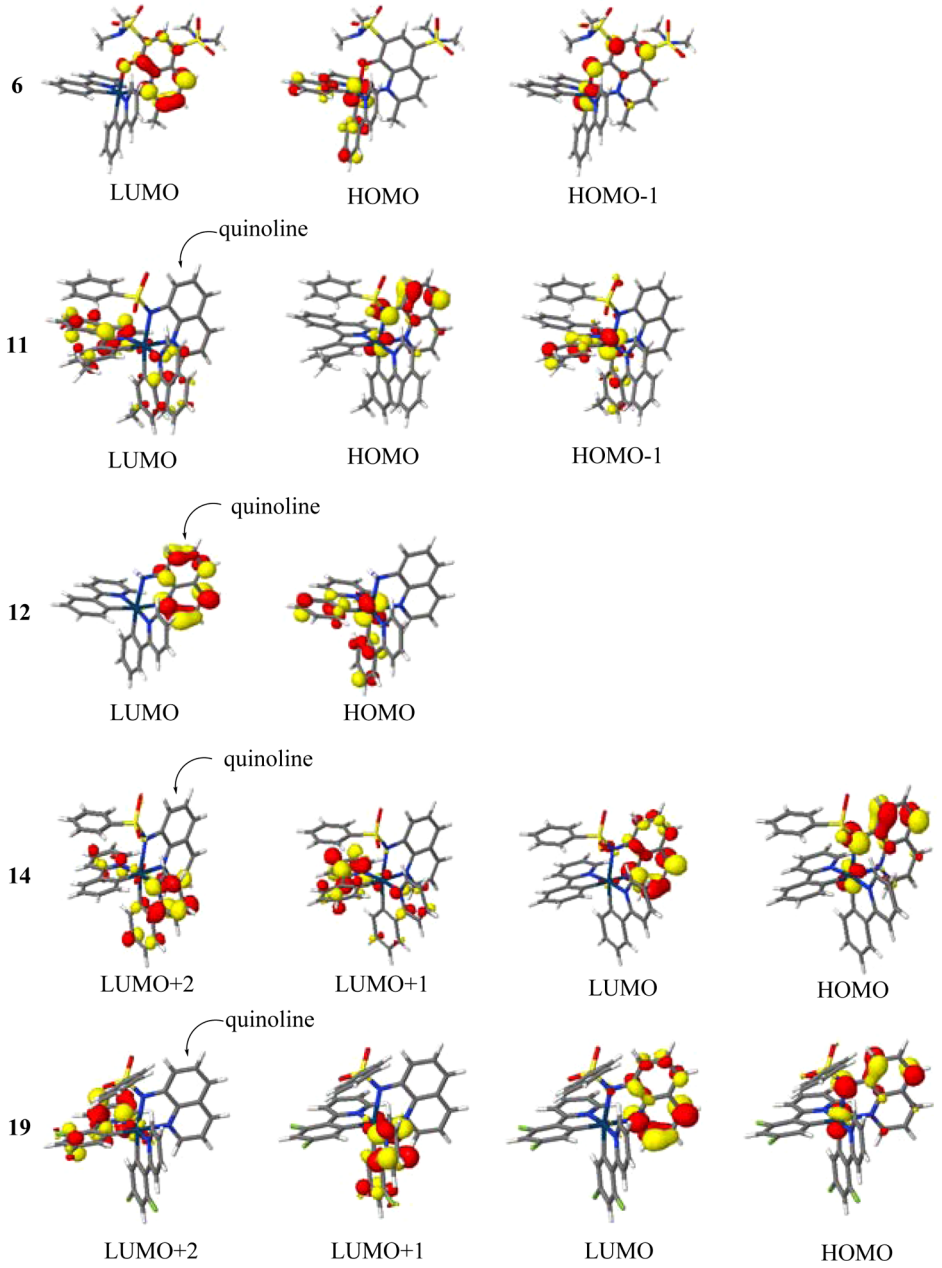

Figure 7. Molecular orbitals of **6**, **11**, **12**, **14**, and **19**.

for $C_{46}H_{42}IrN_5O_5S_2$: C, 55.18; H, 4.23; N, 6.99. Found: C, 55.25, H, 4.11; N, 6.67%.

11: Yield = 92% (38 mg). Yellow color. mp > 300 °C. IR (ATR): ν = 1586, 1501, 1443, 1375, 1311, 1287, 1139, 1110, 1085, 941, 813, 741, 672, 579 cm^{-1}. ^1H NMR (300 MHz, $CDCl_3$) δ 9.05 (d, J = 6.5 Hz, 1H), 8.93 (d, 6.0 Hz, 1H), 8.87 (d, 6.9 Hz, 1H), 8.10 (d, J = 8.0 Hz, 1H), 8.04 (dd, J = 8.2, 3.3 Hz, 2H), 8.01−7.96 (m, 1H), 7.87−7.72 (m, 2H), 7.73−7.58 (m, 4H), 7.56 (dd, J = 4.9, 1.5 Hz, 1H), 7.44 (t, J = 8.1 Hz, 1H), 7.29 (d, J = 6.6 Hz, 2H), 7.17−7.04 (m, 4H), 7.01 (d, J = 6.5 Hz, 1H), 6.92 (t, J = 7.4 Hz, 1H), 6.82 (d, J = 6.7 Hz, 1H), 6.71 (dd, J = 15.3, 7.5 Hz, 3H), 6.16 (d, J = 2.8 Hz, 2H), 2.06 (s, 3H), 2.01 (s, 3H) ppm. ESI-MS (m/z): Calcd for $C_{47}H_{35}N_4O_2S(^{191}Ir)$ (M^+): 910.2081. Found: 910.2097. Anal. Calcd for $C_{47}H_{35}IrN_4O_2S\cdot CH_2Cl_2$: C, 57.82; H, 3.74; N, 5.62. Found: C, 57.77, H, 3.49; N, 5.66%.

12: Yield = 79% (19 mg). Yellow color solid. mp > 300 °C. IR (ATR): ν = 2892, 1608, 1582, 1477, 1421, 1374, 1315, 1270, 1211, 1156, 1062, 1031, 828, 785, 730, 629, 556 cm^{-1}. ^1H NMR (300 MHz, DMSO-d_6) δ 8.69−8.56 (m, 2H), 8.35−8.24 (m, 1H), 8.19 (d, J = 8.3 Hz, 1H), 8.03 (s, 1H), 7.98 (d, J = 6.3 Hz, 2H), 7.84 (t, J = 8.7 Hz, 4H), 7.73 (d, J = 6.9 Hz, 2H), 7.63 (dd, J = 8.4, 4.9 Hz, 1H), 7.17−7.06 (m, 2H), 7.01−6.74 (m, 4H), 6.27 (dd, J = 14.5, 6.5 Hz, 2H) ppm. ESI-MS (m/z): Calcd for $C_{31}H_{24}N_4(^{191}Ir)$ (M^+): 643.1601. Found: 643.1590. Elemental analysis was not carried out because the content of iridium in **12** is >25%.

13: Yield = 71% (24 mg). Yellow color solid. mp > 300 °C. IR (ATR): ν = 1605, 1585, 1653, 1502, 1476, 1311, 1288, 1268, 1126, 1062, 1029, 956, 856, 826, 747, 665, 544, 520 cm^{-1}. ^1H NMR (300 MHz, $CDCl_3$) δ 9.24 (d, J = 4.9 Hz, 1H), 8.16 (d, J = 7.3 Hz, 1H), 8.09−8.00 (m, 1H), 7.92 (d, J = 7.9 Hz, 1H), 7.81 (d, J = 8.3 Hz, 1H), 7.74 (dd, J = 4.9, 1.5 Hz, 1H), 7.68−7.58 (m, 4H), 7.53 (t, J = 8.1 Hz, 1H), 7.25 (s, 1H), 7.21−7.10 (m, 2H), 7.06 (t, J = 6.6 Hz, 1H), 6.83−6.73 (m, 5H), 6.32 (d, J = 7.6 Hz, 1H), 6.23 (d, J = 7.5 Hz, 1H), 2.27 (s, 3H) ppm. ESI-MS (m/z): Calcd for $C_{32}H_{25}N_4O_2S(^{191}Ir)$ (M^+): 720.1299. Found: 720.1303. Anal. Calcd for $C_{32}H_{25}IrN_4O_2S\cdot CHCl_3$: C, 47.12; H, 3.12; N, 6.66. Found: C, 47.07, H, 2.73; N, 6.55%.

14: Yield = 46% (20 mg). Yellow color solid. mp > 300 °C. IR (ATR): ν = 1603, 1582, 1562, 1474, 1416, 1380, 1312, 1262, 1193,

DOI: 10.1021/acs.inorgchem.5b02872
Inorg. Chem. XXXX, XXX, XXX−XXX

Table 6. Calculated Triplet Transition States and Selected Frontier Orbitals of Compounds 6, 8, 10−16, 18−21

	wavelength (nm) expt	*E* (eV) expt	*E* (eV) TD-DFT	state	assignment[a]	main transition character
6	587	2.11	2.23	T_1	HOMO−1→LUMO (80%)	$^3ML_{quin}CT + {}^3L_{quin}C$
8	588	2.10	2.24	T_1	HOMO−1→LUMO (76%)	$^3ML_{quin}CT + {}^3L_{quin}C$
10	600	2.07	2.10	T_1	HOMO→LUMO (54%)	$^3ML_{mpiq}CT + {}^3L_{quin}L_{mpiq}CT$
					HOMO→LUMO+1 (10%)	
11	602	2.06	2.12	T_1	HOMO→LUMO (14%)	$^3ML_{mpiq}CT + {}^3L_{quin}L_{mpiq}CT$
					HOMO−1→LUMO (36%)	$^3L_{mpiq}C$
12	557	2.22	2.09	T_1	HOMO→LUMO (98%)	$^3ML_{ppy}CT + {}^3L_{ppy}L_{quin}CT$
13	500	2.47	2.56	T_1	HOMO→LUMO+1 (20%)	$^3ML_{ppy}CT + {}^3L_{quin}L_{ppy}CT$
					HOMO→LUMO+2 (28%)	
14	617	2.00	1.90	T_1	HOMO→LUMO (88%)	$^3ML_{quin}CT + {}^3L_{quin}C + {}^3IL_{quin}CT$
	496	2.49	2.51	T_2	HOMO→LUMO+1 (44%)	$^3ML_{ppy}CT + {}^3L_{quin}L_{ppy}CT$
					HOMO→LUMO+2 (18%)	
15	611	2.03	1.91	T_1	HOMO→LUMO (88%)	$^3ML_{quin}CT + {}^3L_{quin}C + {}^3IL_{quin}CT$
	496	2.50	2.51	T_2	HOMO→LUMO+1 (36%)	$^3ML_{ppy}CT + {}^3L_{quin}L_{ppy}CT$
					HOMO→LUMO+2 (20%)	
16	622	1.99	1.89	T_1	HOMO→LUMO (92%)	$^3ML_{quin}CT + {}^3L_{quin}C + {}^3IL_{quin}CT$
	500	2.47	2.52	T_2	HOMO→LUMO+1 (48%)	$^3ML_{ppy}CT + {}^3L_{quin}L_{ppy}CT$
					HOMO→LUMO+2 (20%)	
18	617	2.01	1.89	T_1	HOMO→LUMO (92%)	$^3ML_{quin}CT + {}^3L_{quin}C + {}^3IL_{quin}CT$
	487	2.54	2.53	T_2	HOMO→LUMO+1 (26%)	$^3ML_{mppy}CT + {}^3L_{quin}L_{mppy}CT$
					HOMO→LUMO+2 (12%)	
19	613	2.02	2.08	T_1	HOMO→LUMO (84%)	$^3ML_{quin}CT + {}^3L_{quin}C + {}^3IL_{quin}CT$
	474	2.61	2.76	T_2	HOMO→LUMO+1 (84%)	$^3ML_{F2ppy}CT + {}^3L_{quin}L_{F2ppy}CT$
20	617	2.01	1.84	T_1	HOMO→LUMO (86%)	$^3ML_{quin}CT + {}^3L_{quin}C + {}^3IL_{quin}CT$
	476	2.60	2.58	T_2	HOMO→LUMO+1 (36%)	$^3ML_{F2ppy}CT + {}^3L_{quin}L_{F2ppy}CT$
					HOMO→LUMO+2 (16%)	
21	615	2.01	1.90	T_1	HOMO→LUMO (79%)	$^3ML_{quin}CT + {}^3L_{quin}C + {}^3IL_{quin}CT$
	494	2.50	2.47	T_2	HOMO→LUMO+1 (68%)	$^3ML_{F2ppy}CT + {}^3L_{quin}L_{F2ppy}CT$
					HOMO→LUMO+2 (12%)	

[a]Major contributions defined as >10% contribution to the transition.

Scheme 5. Proposed Energy Diagram of 19

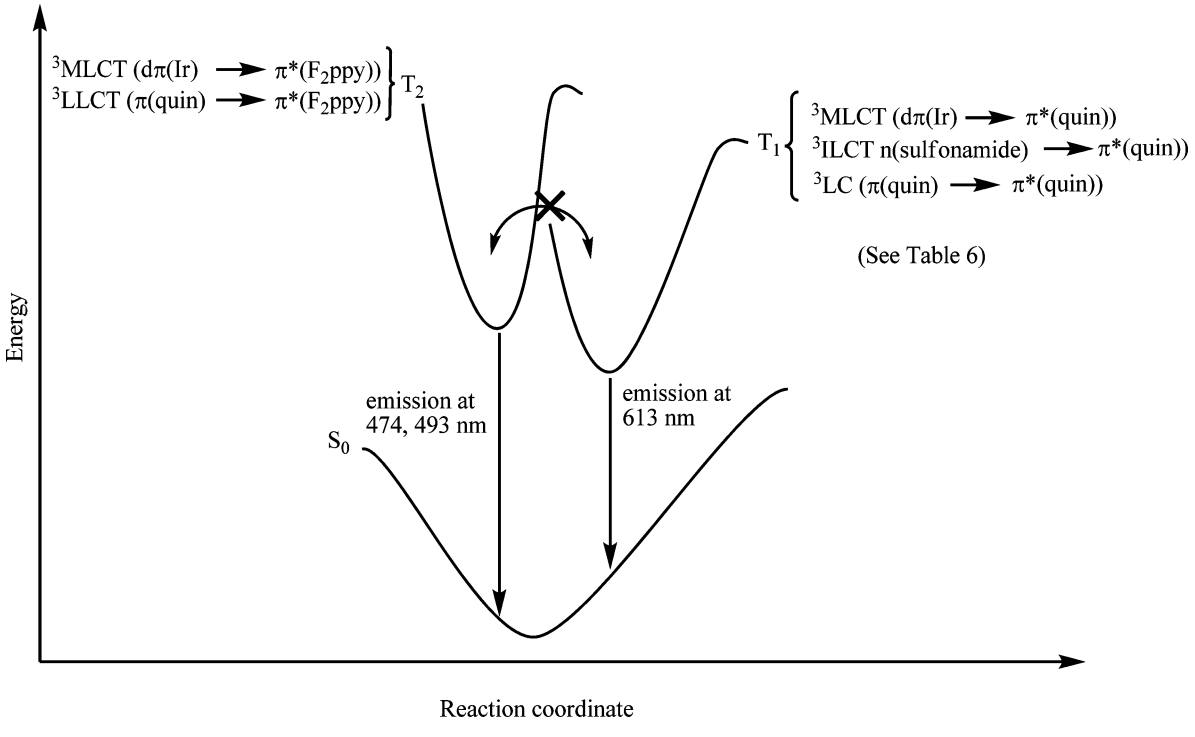

DOI: 10.1021/acs.inorgchem.5b02872
Inorg. Chem. XXXX, XXX, XXX−XXX

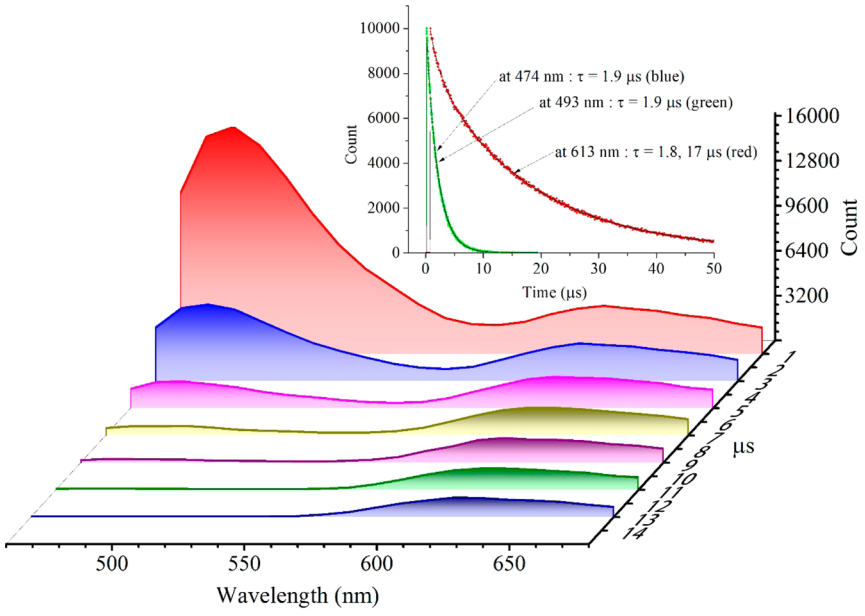

Figure 8. Time-resolved emission spectra of **19** (10 μM) in DMSO at 298 K, excitation 371 nm. (inset) Emission decay curves at 474, 493, and 613 nm.

Table 7. Lifetimes[a] of 14 and 19 in Degassed Dimethyl Sulfoxide at 298 K

comp	emission (nm)	lifetime τ (μs)
14	496 (HEB)	1.7 (100%)[b]
	617 (LEB)	1.3 (4%), 12 (96%)
19	474 (HEB)	1.9 (100%)
	493 (HEB)	1.9 (100%)
	613 (LEB)	1.8 (2%), 17 (98%)

[a]Determined from emission decay curves monitored at each emission wavelength. Excitation at 371 nm. [b]Values in parentheses are distribution of each decay component in the emission intensity at the indicated wavelength.

1139, 1115, 1084, 945, 844, 735, 581 cm^{-1}. ^{1}H NMR (300 MHz, $CDCl_3$) δ 9.23 (d, J = 8.2 Hz, 1H), 8.26 (d, J = 8.4 Hz, 1H), 8.02 (d, J = 8.3 Hz, 1H), 7.76 (dd, J = 7.8, 4.2 Hz, 2H), 7.69–7.59 (m, 2H), 7.56 (d, J = 7.3 Hz, 2H), 7.49–7.36 (m, 2H), 7.13 (dd, J = 8.0, 3.3 Hz, 5H), 7.03 (d, J = 7.8 Hz 1H), 6.99–6.85 (m, 3H), 6.92–6.66 (m, 5H), 6.37 (d, J = 8.8 Hz, 1H), 6.15 (d, J = 7.2 Hz, 1H) ppm. ESI-MS (m/z): Calcd for $C_{37}H_{27}N_4O_2S(^{191}Ir)$ (M^+): 782.1451. Found: 782.1455. Anal. Calcd for $C_{37}H_{27}IrN_4O_2S{\cdot}0.33CHCl_3$: C, 55.21; H, 3.43; N, 6.90. Found: C, 55.60, H, 3.14; N, 6.93%.

15: Yield = 75% (48 mg). Yellow color solid. mp > 300 °C. IR (ATR): ν = 1604, 1571, 1502, 1474, 1417, 1386, 1297, 1268, 1158, 1136, 1058, 1028, 946, 858, 733, 602, 568 cm^{-1}. ^{1}H NMR (300 MHz, $CDCl_3$) δ 9.29 (d, J = 5.7 Hz, 1H), 8.45 (d, J = 8.1 Hz, 1H), 8.05 (d, J = 8.3 Hz, 2H), 7.79 (d, J = 8.5 Hz, 2H), 7.72–7.66 (m, 2H), 7.62–7.51 (m, 2H), 7.39 (s, 2H), 7.23–7.09 (m, 4H), 7.00 (d, J = 8.5 Hz, 2H), 6.95–6.86 (m, 2H), 6.85–6.73 (m, 2H), 6.69 (s, 2H), 6.38 (d, J = 6.9 Hz, 1H), 6.06 (d, J = 7.5 Hz, 1H) ppm. ESI-MS (m/z): Calcd for $C_{37}H_{26}BrN_4O_2S$ (^{191}Ir) (M^+): 860.0560. Found: 860.0570. Anal. Calcd for $C_{37}H_{26}IrN_4O_2S{\cdot}CHCl_3$: C, 46.47; H, 2.77; N, 5.70. Found: C, 46.69, H, 2.52; N, 5.66%.

16: Yield = 64% (38 mg). Yellow color solid. mp > 300 °C. IR (ATR): ν = 1603, 1581, 1497, 1475, 1257, 1418, 1381, 1311, 1253, 1160, 1138, 1088, 1029, 942, 823, 761, 679, 628, 573 cm^{-1}. ^{1}H NMR (300 MHz, $CDCl_3$) δ 9.26 (d, J = 6.0 Hz, 1H), 8.26 (d, J = 8.2 Hz, 1H), 8.02 (d, J = 8.3 Hz, 1H), 7.84–7.69 (m, 3H), 7.69–7.52 (m, 4H), 7.47 (t, J = 8.1 Hz, 2H), 7.17–7.07 (m, 2H), 7.03 (dd, J = 5.5, 3.4 Hz, 3H), 6.92 (t, J = 7.0 Hz, 1H), 6.87–6.61 (m, 4H), 6.49–6.31 (m, 3H), 6.15 (d, J = 7.4 Hz, 1H), 3.74 (s, J = 4.7 Hz, 3H) ppm. ESI-MS (m/z): Calcd for $C_{38}H_{29}N_4O_3S$ (^{191}Ir) (M^+): 812.1561. Found: 812.1563. Anal. Calcd for $C_{38}H_{29}IrN_4O_3S$: C, 56.07; H, 3.59; N, 6.88. Found: C, 55.69, H, 3.27; N, 6.74%.

17: Yield = 72% (45 mg). Yellow color solid. mp > 300 °C. IR (ATR): ν = 1604, 1581, 1561, 1496, 1475, 1456, 1417, 1380, 1309, 1286, 1262, 1191, 1119, 1061, 944, 847, 759, 593. 576 cm^{-1}. ^{1}H NMR (300 MHz, $CDCl_3$) δ 9.58 (d, J = 5.1 Hz, 1H), 9.30 (d, J = 7.4 Hz, 1H), 8.41–8.33 (m, 1H), 8.03 (dd, J = 8.3, 1.5 Hz, 1H), 7.81 (dd, J = 8.3, 1.8 Hz, 1H), 7.72 (t, J = 8.2 Hz, 2H), 7.65–7.56 (m, 2H), 7.52–7.49 (m, 2H), 7.22 (d, J = 6.9 Hz, 1H), 7.17–6.88 (m, 8H), 6.88–6.72 (m, 4H), 6.66 (t, J = 6.8 Hz, 1H), 6.38 (s, 1H), 5.93 (s, 1H), 5.83 (d, J = 7.7 Hz, 1H) ppm. ESI-MS (m/z): Calcd for $C_{40}H_{28}N_5O_2S(^{191}Ir)$ ($M+H^+$): 834.1642. Found: 834.1642. Anal. Calcd for $C_{40}H_{28}IrN_5O_2S{\cdot}0.5CHCl_3$: C, 54.37; H, 3.21; N, 7.83. Found: C, 54.70, H, 3.07; N, 7.62%.

18: Yield = 75% (21 mg). Yellow color solid. mp > 300 °C. IR (ATR): ν = 1590, 1548, 1460, 1427, 1311, 1275, 1213, 1143, 1108, 1085, 1036, 944, 860, 819, 774, 744, 713, 690, 582 cm^{-1}. ^{1}H NMR (300 MHz, $CDCl_3$) δ 9.12 (d, J = 4.9 Hz, 1H), 8.17 (d, J = 8.4 Hz, 1H), 8.01 (d, J = 8.3 Hz, 1H), 7.79 (d, J = 5.1 Hz, 1H), 7.67–7.55 (m, 3H), 7.55–7.45 (m, 3H), 7.45–7.37 (m, 2H), 7.18 (d, J = 8.2 Hz, 3H), 7.12 (dd, J = 8.1, 4.9 Hz, 2H), 7.01–6.91 (m, 3H), 6.63 (s, 1H), 6.51 (dd, J = 8.3, 2.6 Hz, 1H), 6.44 (dd, J = 8.5, 2.6 Hz, 1H), 5.83 (d, J = 2.6 Hz, 1H), 5.72 (d, J = 2.6 Hz, 1H), 3.57 (s, 3H), 3.55 (s, 3H) ppm. ESI-MS (m/z): Calcd for $C_{39}H_{31}N_4O_4S(^{191}Ir)$ (M^+): 842.1666. Found: 842.1674. Anal. Calcd for $C_{39}H_{31}IrN_4O_2S{\cdot}CHCl_3$: C, 48.87; H, 3.35; N, 5.82. Found: C, 48.59, H, 3.73; N, 5.86%.

19: Yield = 97% (68 mg). Yellow color solid. mp > 300 °C. IR (ATR): ν = 1601, 1569, 1477, 1459, 1401, 1310, 1295, 1247, 1161, 1143, 1086, 987, 945, 842, 823, 754, 715, 689, 567 cm^{-1}. ^{1}H NMR (300 MHz, $CDCl_3$) δ 9.20 (dd, J = 5.9, 1.0 Hz, 1H), 8.27 (dd, J = 8.2, 0.8 Hz, 1H), 8.19 (d, J = 8.3 Hz, 1H), 8.08 (dt, J = 7.7, 3.9 Hz, 2H), 7.74 (dd, J = 4.9, 1.5 Hz, 1H), 7.69 (t, J = 8.2 Hz, 1H), 7.60 (t, J = 8.4 Hz, 1H), 7.49 (t, J = 8.1 Hz, 1H), 7.25–7.22 (m, 1H), 7.22–7.12 (m, 4H), 7.06 (ddd, J = 7.3, 5.9, 1.3 Hz, 1H), 7.00 (t, J = 7.8 Hz, 2H), 6.80–6.70 (m, 1H), 6.49 (t, J = 7.9 Hz, 1H), 6.52–6.43 (m, 1H), 6.37–6.25 (m, 1H), 5.72 (dd, J = 8.1, 2.3 Hz, 1H), 5.58 (dd, J = 8.2, 2.3 Hz, 1H) ppm. ESI-MS (m/z): Calcd for $C_{37}H_{23}F_4N_4O_2S(^{191}Ir)$ (M^+): 854.1078. Found: 854.1066. Elemental analysis was not carried out because the content of fluorine in **19** is >25%.

20: Yield = 69% (37 mg). Yellow color solid. mp > 300 °C. IR (ATR): ν = 1599, 1573, 1497, 1477, 1402, 1310, 1291, 1260, 1246, 1136, 1101, 1085, 985, 945, 859, 825, 782, 753, 663, 574 cm^{-1}. ^{1}H

DOI: 10.1021/acs.inorgchem.5b02872
Inorg. Chem. XXXX, XXX, XXX–XXX

NMR (300 MHz, $CDCl_3$) δ 9.24 (d, J = 5.7 Hz, 1H), 8.31 (d, J = 8.1 Hz, 1H), 8.20 (d, J = 7.5 Hz, 1H), 8.07 (s, 2H), 7.77−7.56 (m, 3H), 7.50 (t, J = 8.1 Hz, 1H), 7.24−7.12 (m, 3H), 7.11−6.97 (m, 3H), 6.77 (t, J = 6.2 Hz, 1H), 6.46 (d, J = 8.1 Hz, 3H), 6.36 (m, 1H), 5.73 (d, J = 8.0 Hz, 1H), 5.56 (d, J = 6.5 Hz, 1H), 3.75 (d, J = 6.1 Hz, 3H) ppm. ESI-MS (m/z): Calcd for $C_{38}H_{25}F_4N_4O_3S(^{191}Ir)$ (M^+): 884.1184. Found: 884.1206. Elemental analysis was not performed because the content of fluorine in **20** is >25%.

21: Yield = 49% (26 mg). Yellow color solid. mp > 300 °C. IR (ATR): ν = 1601, 1568, 1557, 1504, 1476, 1402, 1310, 1245, 1291, 1126, 1101, 985, 957, 843, 824, 748, 568, 548, 523 cm^{-1}. ^1H NMR (300 MHz, $CDCl_3$) δ 9.15 (d, J = 4.8 Hz, 1H), 8.34 (d, J = 8.6 Hz, 1H), 8.21 (d, J = 8.1 Hz, 1H), 8.13 (dd, J = 7.8, 4.6 Hz, 2H), 7.80−7.64 (m, 3H), 7.56 (t, J = 8.1 Hz, 1H), 7.25 (s, 1H), 7.22 (dd, J = 8.3, 3.4 Hz, 2H), 7.09 (t, J = 6.7 Hz, 1H), 6.80 (t, J = 6.7 Hz, 1H), 6.54−6.28 (m, 2H), 5.67 (ddd, J = 15.5, 8.7, 2.3 Hz, 2H), 2.29 (s, J = 6.5 Hz, 3H) ppm. ESI-MS (m/z): Calcd for $C_{32}H_{21}F_4N_4O_2S(^{191}Ir)$ (M^+): 792.0917. Found: 792.0910. Elemental analysis was not carried out because the content of fluorine in **21** is >25%.

X-ray Data Collection and Refinement. Single-crystal X-ray studies were performed on a Bruker APEX II CCD diffractometer equipped with a Bruker Instruments low-temperature attachment. Data were collected at 100 K using graphite-monochromated Mo Kα radiation (λ = 0.710 73 Å). The frames were indexed, integrated, and scaled using the SMART and SAINT software packages.[33] An empirical absorption correction was applied to the collected reflections with SADABS[34] using XPREP.[35] All of the structures were solved by the direct method using the program SHELXS-97 and were refined on F^2 by the full-matrix least squares technique using the SHELXL-97 program package.[36] All non-hydrogen atoms were refined anisotropically in the structure.

Crystal Data for ***14****.* $C_{37}H_{27}IrN_4O_2S{\cdot}CHCl_3$, Mr = 903.27, monoclinic, $P21/n$, a = 19.194(5), b = 9.114(5), c = 19.709(5) Å, α = 90, β = 101.926(5), γ = 90°, V = 3374(2) $Å^3$, Z = 4, $\rho_{calc=}$ 1.778 $g.cm^{-3}$, R = 0.0280 (for 5349 reflection with $I > 2\sigma(I)$), Rw = 0.0656 (for 6166 reflections), GOF = 0.996. CCDC 1439264 contains the supplementary crystallographic data for the compound. Additional crystallographic information is available in the Supporting Information.

Crystal Data for ***19****.* $C_{37}H_{23}F_4IrN_4O_2S{\cdot}CHCl_3$, Mr = 975.22, Triclinic, $P\bar{1}$, a = 11.477(5), b = 13.075(5), c = 13.777(5) Å, α = 73.813(5), β = 71.921(5), γ = 66.201(5)°, V = 1770.0(12) $Å^3$, Z = 2, ρ_{calc} = 1.830 $g.cm^{-3}$, R = 0.0435 (for 6326 reflection with $I > 2\sigma(I)$), Rw = 0.1096 (for 7103 reflections), GOF = 1.038. CCDC 1439265 contains the supplementary crystallographic data for the compound.

Crystal Data for ***20****.* $C_{38}H_{25}F_4IrN_4O_3S$, Mr = 885.88, monoclinic, $P\bar{1}$, a = 10.355(5), b = 11.129(5), c = 16.199(5) Å, α = 85.020, β = 77.980(5), γ = 84.218(5) °, V = 1812(13) $Å^3$, Z = 2, $\rho_{calc=}$ 1.623 $g{\cdot}cm^{-3}$, R = 0.0336 (for 5874 reflection with $I > 2\sigma(I)$), Rw = 0.0826 (for 6602 reflections), GOF = 1.042. CCDC 1439266 contains the supplementary crystallographic data for the compound.

Measurements of Ultraviolet−Visible Absorption and Luminescence Spectra. UV−vis spectra were recorded on a JASCO V-550 UV−vis spectrophotometer, and emission spectra were recorded on a JASCO FP-6200 and FP-6500 spectrofluorometer, respectively. Sample solutions in quartz cuvettes equipped with Teflon septum screw caps were degassed by bubbling Ar through the solution for 10 min prior to making the luminescence measurements. The quantum yields for luminescence (Φ) were determined by comparison with the integrated corrected emission spectrum of $Ir(mpiq)_3$ (**2**) (Φ = 0.26).[22] Equation 1 was used to calculate the emission quantum yields, in which Φ_s and Φ_r denote the quantum yields of the sample and reference compound, η_s and η_r are the refractive indexes of the solvents used for the measurements of the sample and the reference (1.477 for DMSO (η_s)), A_s and A_r are the absorbance of the sample and the reference, and I_s and I_r stand for the integrated areas under the emission spectra of the sample and reference, respectively (all of the Ir compounds were excited at 366 nm for luminescence measurements in this study). For the determination of Φ_s in mixed-solvent systems, the η values of the main solvents were used for the calculation.

$$\Phi_s = \Phi_r(\eta_s^2 A_r I_s)/(\eta_r^2 A_s I_r) \quad (1)$$

The luminescence lifetimes of sample solutions of Ir(III) complexes in degassed DMSO at 298 K were measured on a TSP1000-M-PL (Unisoku, Osaka, Japan) instrument by using THG (355 nm) of Nd:YAG laser, Minilite I (Continuum, CA, USA) as excitation source and long wave pass filters (435 nm, 475 or 550 nm). The signals were monitored with an R2949 photomultiplier. Data were analyzed using a single exponential decay equation. Sample solutions in quartz cuvettes equipped with Teflon septum screw caps were degassed by bubbling Ar through the solution for 20 min prior to measuring the lifetime.

Time-Resolved Emission Spectroscopy. Emission decay was measured at emission maxima corresponding to the emission from Ir(III) complexes by the time-dependent single photon counting method using a FluoroCube 1000U−S spectrofluorometer under 371 nm photoexcitation (NanoLED-440L, HORIBA) with a TBX-04 detector at 298 K.

■ ASSOCIATED CONTENT

Supporting Information

The Supporting Information is available free of charge on the ACS Publications website at DOI: 10.1021/acs.inorgchem.5b02872. Related crystallographic data can be obtained free of charge from The Cambridge Crystallographic Data Centre via www.ccdc.cam.ac.uk/data_request/cif.

UV−vis spectra of **11**−**21**, excitation spectra of **11**, **14**, **19**, emission spectra of **14** in different solvents, emission spectra of **19** at different temperatures, solid-state emission spectra of **13**−**17**, emission spectra of **11**, **14**, **19** of doped PMMA film, emission decay graphs of **11** and **14**. (PDF)

X-ray crystallographic files of **14**, **19**, and **20**. (CIF)

■ AUTHOR INFORMATION

Corresponding Author

*E-mail: shinaoki@rs.noda.tus.ac.jp. Phone: +81-4-7121-3670.

Notes

The authors declare no competing financial interest.

■ ACKNOWLEDGMENTS

This work is supported by the Grants-in-Aid from the Ministry of Education, Culture, Sports, Science and Technology (MEXI) of Japan (No. 26860016 for Y.H. and Nos. 24659055 and 24640156 for S.A). We thank Mr. S. Ootsu and Mr. N. Ueda (Konica Minolta Holding, Inc. Japan) for helpful discussions. We wish to acknowledge Mrs. F. Hasegawa (Faculty of Pharmaceutical Science, Tokyo University of Science) for measurement of mass spectra and Ms. T. Mastsuo (Research Institute for Science and Technology, Tokyo University of Science) for the X-ray single-crystal structure analysis.

■ REFERENCES

(1) Forrest, S. R.; Thompson, M. E.; Baldo, M. A. *Nature* **2000**, *403*, 750−753.

(2) (a) Tamayo, A. B.; Alleyne, B. D.; Djurovich, P. I.; Lamansky, S.; Tsyba, I.; Ho, N. N.; Bau, R.; Thompson, M. E. *J. Am. Chem. Soc.* **2003**, *125*, 7377−7387. (b) Swanick, K. N.; Ladouceur, K.; Zysman-Colman, E.; Ding, Z. *Angew. Chem., Int. Ed.* **2012**, *51*, 11079−11082. (c) Hisamatsu, Y.; Aoki, S. *Eur. J. Inorg. Chem.* **2011**, *2011*, 5360−5369. (d) Wong, W.-Y.; Ho, C.-L. *Coord. Chem. Rev.* **2009**, *253*, 1709−1758. (e) Ulbricht, C.; Beyer, B.; Friebe, C.; Winter, A.; Schubert, U. S. *Adv. Mater.* **2009**, *21*, 4418−4441. and reference cited therein. (f) Sudhakar, M.; Djurovich, P. I.; Hogen-Esch, T. E.; Thompson, M. E. *J. Am. Chem. Soc.* **2003**, *125*, 7796−7797. (g) Chi, Y.; Chou, P.-T.

DOI: 10.1021/acs.inorgchem.5b02872
Inorg. Chem. XXXX, XXX, XXX−XXX

Chem. Soc. Rev. **2010**, *39*, 638−655. (h) You, Y.; Park, S. Y. *Dalton Trans.* **2009**, 1267−1282.
(3) (a) Zhuang, J.; Li, W.; Wu, W.; Song, M.; Su, W.; Zhou, M.; Cui, Z. *New J. Chem.* **2015**, *39*, 246−253. (b) Bolink, H. J.; De Angelis, F.; Baranoff, E.; Klein, C.; Fantacci, S.; Coronado, E.; Sessolo, M.; Kalyanasundaram, K.; Gratzel, M.; Nazeeruddin, Md. K. *Chem. Commun.* **2009**, 4672−4674. (c) Lowry, M. S.; Bernhard, S. *Chem. - Eur. J.* **2006**, *12*, 7970−7977. (d) Friend, R. H.; Gymer, R. W.; Holmes, A. B.; Burroughes, J. H.; Marks, R. N.; Taliani, C.; Bradley, D. D. C.; Dos Santos, D. A.; Brdas, J. L.; Lgdlund, M.; Salaneck, W. R. *Nature* **1999**, *397*, 121−128.
(4) (a) Zhao, Q.; Huang, C.; Li, F. *Chem. Soc. Rev.* **2011**, *40*, 2508−2524. (b) Lo, K. K.-W.; Louie, M.-W.; Zhang, K. Y. *Coord. Chem. Rev.* **2010**, *254*, 2603−2622. (c) Zhang, K. Y.; Li, S. P.-Y.; Zhu, N.; Or, I. W.-S.; Cheung, M. S.-H.; Lam, Y.-W.; Lo, K.K.-W. *Inorg. Chem.* **2010**, *49*, 2530−2540. (d) Leung, S.-K.; Kwok, K. Y.; Zhang, K. Y.; Lo, K.K.-W. *Inorg. Chem.* **2010**, *49*, 4984−4995. (e) Zhang, K. Y.; Liu, H.-W.; Fong, T. T.-H.; Chen, X.-G.; Lo, K.K.-W. *Inorg. Chem.* **2010**, *49*, 5432−5443. (f) Zhao, Q.; Yu, M.; Shi, L.; Liu, S.; Li, C.; Shi, M.; Zhou, Z.; Huang, C.; Li, F. *Organometallics* **2010**, *29*, 1085−1091. (g) DeRosa, M. C.; Hodgson, D. J.; Enright, G. D.; Dawson, B.; Evans, C. E. B.; Crutchley, R. J. *J. Am. Chem. Soc.* **2004**, *126*, 7619−7626. (h) You, Y.; Cho, S.; Nam, W. *Inorg. Chem.* **2014**, *53*, 1804−1815. and reference cited therein. (i) Patra, M.; Gasser, G. *ChemBioChem* **2012**, *13*, 1232−1252. (j) You, Y.; Nam, W. *Chem. Soc. Rev.* **2012**, *41*, 7061−7084. (k) Lo, K. K.-W.; Tso, K. K.-S. *Inorg. Chem. Front.* **2015**, *2*, 510−524. (l) Lo, K. K.-W.; Zhang, K. Y. *RSC Adv.* **2012**, *2*, 12069−12083. (m) Baggaley, E.; Weinstein, J. A.; Williams, J. A. G. *Coord. Chem. Rev.* **2012**, *256*, 1762−1785.
(5) (a) Aoki, S.; Matsuo, Y.; Ogura, S.; Ohwada, H.; Hisamatsu, Y.; Moromizato, S.; Shiro, M.; Kitamura, M. *Inorg. Chem.* **2011**, *50*, 806−818. (b) Moromizato, S.; Hisamatsu, Y.; Suzuki, T.; Matsuo, Y.; Abe, R.; Aoki, S. *Inorg. Chem.* **2012**, *51*, 12697−12706. (c) Nakagawa, A.; Hisamatsu, Y.; Moromizato, S.; Kohno, M.; Aoki, S. *Inorg. Chem.* **2014**, *53*, 409−422. (d) Kando, A.; Hisamatsu, Y.; Ohwada, H.; Itoh, T.; Moromizato, S.; Kohno, M.; Aoki, S. *Inorg. Chem.* **2015**, *54*, 5342−5357. (e) Licini, M.; Gareth Williams, J. A. *Chem. Commun.* **1999**, 1943−1944. (f) Arm, K. J.; Leslie, W.; Williams, J. A. G. *Inorg. Chim. Acta* **2006**, *359*, 1222−1232. (g) Chen, Y.; Zhang, A.; Liu, Y.; Wang, K. *J. Organomet. Chem.* **2011**, *696*, 1716−1722. (h) Weng, J.; Mei, Q.; Jiang, W.; Fan, Q.; Tong, B.; Ling, Q.; Huang, W. *Analyst* **2013**, *138*, 1689−1699. (i) He, L.; Tan, C.-P.; Ye, R.-R.; Zhao, Y.-Z.; Liu, Y.-H.; Zhao, Q.; Ji, L.-N.; Mao, Z.-W. *Angew. Chem., Int. Ed.* **2014**, *53*, 12137−12141. (j) Zhang, Q.; Zhou, M. *Talanta* **2015**, *131*, 666−671. (k) Murphy, L.; Congreve, A.; Palsson, L.-O.; Williams, J. A. G. *Chem. Commun.* **2009**, *46*, 8743−8745. (l) Goldstein, D. C.; Cheng, Y. Y.; Schmidt, T. W.; Bhadbhade, M.; Thordarson, P. *Dalton Trans.* **2011**, *40*, 2053−2061.
(6) (a) Liu, C.; Lv, X.; Xing, Y.; Qiu, J. *J. Mater. Chem. C* **2015**, *3*, 8010−8017. (b) Marín-Suárez, M.; Curchod, B. F. E.; Tavernelli, I.; Rothlisberger, U.; Scopelliti, R.; Jung, I.; Di Censo, D.; Grätzel, M.; Fernández-Sánchez, J. F.; Fernández-Gutiérrez, A.; Nazeeruddin, M. K.; Baranoff, E. *Chem. Mater.* **2012**, *24*, 2330−2338. (c) Takizawa, S.; Aboshi, R.; Murata, S. *Photochem. Photobiol. Sci.* **2011**, *10*, 895−903. (d) Gao, R.; Ho, D. G.; Hernandez, B.; Selke, M.; Murphy, D.; Djurovich, P. I.; Thompson, M. E. *J. Am. Chem. Soc.* **2002**, *124*, 14828−14829. (e) Sun, J.; Zhao, J.; Guo, H.; Wu, W. *Chem. Commun.* **2012**, *48*, 4169−4171. (f) Xue, F.; Lu, Y.; Zhou, Z.; Shi, M.; Yan, Y.; Yang, H.; Yang, S. *Organometallics* **2015**, *34*, 73−77. (g) Li, S. P.-Y.; Lau, C. T.-S.; Louie, M.-W.; Lam, Y.-W.; Lo, K. K.-W. *Biomaterials* **2013**, *34*, 7519−7532. (h) Djurovich, P. I.; Murphy, D.; Thompson, M. E.; Hernandez, B.; Gao, R.; Hunt, P. L.; Selke, M. *Dalton Trans.* **2007**, *34*, 3763−3770. (i) Ashen-Garry, D.; Selke, M. *Photochem. Photobiol.* **2014**, *90*, 257−274. (j) Ye, R.-R.; Tan, C.-P.; He, L.; Chen, M.-H.; Ji, L.-N.; Mao, Z.-W. *Chem. Commun.* **2014**, *50*, 10945−10948. (k) Maggioni, D.; Galli, M.; D'Alfonso, L.; Inverso, D.; Dozzi, M. V.; Sironi, L.; Iannacone, M.; Collini, M.; Ferruti, P.; Ranucci, E.; D'Alfonso, G. *Inorg. Chem.* **2015**, *54*, 544−553. (l) Colombo, A.; Dragonetti, C.; Roberto, D.; Valore, A.; Ferrante, C.; Fortunati, I.; Picone, A. L.; Todescato, F.; Williams, J. A. G. *Dalton Trans.* **2015**, *44*, 15712−15720.
(7) (a) Hisamatsu, Y.; Shibuya, A.; Suzuki, N.; Suzuki, T.; Abe, R.; Aoki, S. *Bioconjugate Chem.* **2015**, *26*, 857−879. (b) Liu, Z.; Salassa, L.; Habtemariam, A.; Pizarro, A. M.; Clarkson, G. J.; Sadler, P. J. *Inorg. Chem.* **2011**, *50*, 5777−5783. (c) Liu, Z.; Sadler, P. J. *Acc. Chem. Res.* **2014**, *47*, 1174−1185.
(8) (a) Huo, H.; Shen, X.; Wang, C.; Zhang, L.; Rose, P.; Chen, L.-N.; Harms, K.; Marsch, M.; Hilt, G.; Meggers, E. *Nature* **2014**, *515*, 100−103. (b) Ma, J.; Ding, X.; Hu, Y.; Huang, Y.; Gong, L.; Meggers, E. *Nat. Commun.* **2014**, *5*, 5531. (c) Chen, L-An.; Tang, X.; Xi, J.; Xu, W.; Gong, L.; Meggers, E. *Angew. Chem., Int. Ed.* **2013**, *52*, 14021−14025.
(9) D'Andrade, B. W.; Forrest, R. S. *Adv. Mater.* **2004**, *16*, 1585−1595.
(10) (a) Sun, C.-Y.; Wang, X.-L.; Zhang, X.; Qin, C.; Li, P.; Su, Z.-M.; Zhu, D.-X.; Shan, G.-G.; Shao, K.-Z.; Wu, H.; Li, J. *Nat. Commun.* **2013**, *4*, 2717. (b) Farinola, G. M.; Ragni, R. *Chem. Soc. Rev.* **2011**, *40*, 3467−3482.
(11) (a) Yeh, Y.-S.; Cheng, Y.-M.; Chou, P.-T.; Lee, G.; Yang, C.-H.; Chi, Y.; Shu, C.-F.; Wang, C.-H. *ChemPhysChem* **2006**, *7*, 2294−2297. (b) Lee, Y. H.; Park, G. Y.; Kim, Y. S. *J. Korean Phys. Soc.* **2007**, *50*, 1722−1728. (c) Lo, K.K.-W.; Zhang, K. Y.; Leung, S.-K.; Tang, M.-C. *Angew. Chem., Int. Ed.* **2008**, *47*, 2213−2216. (d) You, Y.; Han, Y.; Lee, Y.-M.; Park, S. Y.; Nam, W.; Lippard, S. J. *J. Am. Chem. Soc.* **2011**, *133*, 11488−11491. (e) You, Y.; Lee, S.; Kim, T.; Ohkubo, K.; Chae, W.-S.; Fukuzumi, S.; Nam, W.; Lippard, S. J. *J. Am. Chem. Soc.* **2011**, *133*, 18328−18342. (f) Ladouceur, S.; Donato, L.; Romain, M.; Mudraboyina, B. P.; Johansen, M. B.; Wisner, J. A.; Zysman-Colman, E. *Dalton Trans.* **2013**, *42*, 8838−8847. (g) Zhang, K. Y.; Liu, H.-W.; Tang, M.-C.; Choi, A. W.-T.; Zhu, N.; Wei, X.-G.; Lau, K.-C.; Lo, K. K.-W. *Inorg. Chem.* **2015**, *54*, 6582−6593.
(12) (a) Tang, C. W.; Van-Slyke, S. A. *Appl. Phys. Lett.* **1987**, *51*, 913−915. (b) Wang, S. *Coord. Chem. Rev.* **2001**, *215*, 79−98.
(13) (a) Mishra, A.; Nayak, P. K.; Periasamy, N. *Tetrahedron Lett.* **2004**, *45*, 6265−6268. (b) Li, L.; Xu, B. *Tetrahedron* **2008**, *64*, 10986−10995. (c) Fazaeli, Y.; Amini, M. M.; Mohajerani, E.; Sharbatdaran, M.; Torabi, N. *J. Colloid Interface Sci.* **2010**, *346*, 384−390.
(14) (a) Perez-Bolivar, C.; Montes, V. A.; Anzenbacher, P., Jr. *Inorg. Chem.* **2006**, *45*, 9610−9612. (b) Pohl, R.; Montes, V. A.; Shinar, J.; Anzenbacher, P., Jr *J. Org. Chem.* **2004**, *69*, 1723−1725. (c) Pohl, R.; Anzenbacher, P., Jr *Org. Lett.* **2003**, *5*, 2769−2772.
(15) (a) Kappaun, S.; Sax, S.; Eder, S.; Moller, K. C.; Waich, K.; Niedermair, F.; Saf, R.; Mereiter, K.; Jacob, J.; Mullen, K.; List, E. J. W.; Slugovc, C. *Chem. Mater.* **2007**, *19*, 1209−1211. (b) Kappaun, S.; Eder, S.; Sax, S.; Mereiter, K.; List, E. J. W.; Slugovc, C. *Eur. J. Inorg. Chem.* **2007**, *2007*, 4207−4215.
(16) (a) Song, Y.; Xu, H.; Chen, W.; Zhan, P.; Liu, X. *MedChemComm* **2015**, *6*, 61−74. (b) Prajapati, S. M.; Patel, K. D.; Vekariya, R. H.; Panchal, S. N.; Patel, H. D. *RSC Adv.* **2014**, *4*, 24463−24476. (c) Pandeya, S. N.; Tyagi, A. *Int. J. Pharm. Pharmaceu. Sci.* **2011**, *3*, 53−61. (d) Amit, C.; Payal, C.; Kuldeep, K.; Mansimran, S.; Sunaina; Poonam; Kuldeep, S. *Can. Open Pharm. J.* **2014**, *1*, 1−12. (e) Gopaul, K.; Shintre, S. A.; Koorbanally, N. A. *Anti-Cancer Agents Med. Chem.* **2015**, *15*, 631−646.
(17) (a) Aoki, S.; Sakurama, K.; Matsuo, N.; Yamada, Y.; Takasawa, R.; Tanuma, S.-I.; Shiro, M.; Takeda, K.; Kimura, E. *Chem. - Eur. J.* **2006**, *12*, 9066−9080. (b) Ohshima, R.; Kitamura, M.; Shiro, M.; Morita, A.; Ikekita, M.; Kimura, E.; Aoki, S. *Inorg. Chem.* **2010**, *49*, 888−899. (c) Aoki, S.; Sakurama, K.; Ohshima, R.; Matsuo, N.; Yamada, Y.; Takasawa, R.; Tanuma, S.-I.; Takeda, K.; Kimura, E. *Inorg. Chem.* **2008**, *47*, 2747−2754. (d) Hanaya, K.; Suetsugu, M.; Saijo, S.; Yamato, I.; Aoki, S. *JBIC, J. Biol. Inorg. Chem.* **2012**, *17*, 517−529. (e) Ariyasu, S.; Mizuseda, Y.; Hanaya, K.; Aoki, S. *Chem. Pharm. Bull.* **2014**, *62*, 642−648. (f) Hanaya, K.; Yoshioka, S.; Ariyasu, S.; Aoki, S.; Shoji, M.; Sugai, T. *Bioorg. Med. Chem. Lett.* **2016**, *26*, 545−550. (g) Ariyasu, S.; Sawa, A.; Morita, A.; Hanaya, K.; Hoshi, M.; Takahashi, I.; Wang, B.; Aoki, S. *Bioorg. Med. Chem.* **2014**, *22*, 3891−3905. (h) Morita, A.; Ariyasu, S.; Wang, B.; Asanuma, T.; Onoda, T.;

DOI: 10.1021/acs.inorgchem.5b02872
Inorg. Chem. XXXX, XXX, XXX−XXX

Sawa, A.; Tanaka, K.; Takahashi, I.; Togami, S.; Nenoi, M.; Inaba, T.; Aoki, S. *Biochem. Biophys. Res. Commun.* **2014**, *450*, 1498−1504.
(18) Kageyama, Y.; Ohshima, R.; Sakurama, K.; Fujiwara, Y.; Tanimoto, Y.; Yamada, Y.; Aoki, S. *Chem. Pharm. Bull.* **2009**, *57*, 1257−1266.
(19) (a) Sprouse, S.; King, K. A.; Spellane, P. J.; Watts, R. J. *J. Am. Chem. Soc.* **1984**, *106*, 6647−6653. (b) Agarwal, N.; Nayak, P. K. *Tetrahedron Lett.* **2008**, *49*, 2710−2713. (c) Yang, C. H.; Beltran, J.; Lemaur, V.; Cornil, J.; Hartmann, D.; Sarfert, W.; Frohlich, R.; Bizzarri, C.; De Cola, L. *Inorg. Chem.* **2010**, *49*, 9891−9901.
(20) Lamansky, S.; Djurovich, P.; Murphy, D.; Abdel-Razzaq, F.; Kwong, R.; Tsyba, I.; Bortz, M.; Mui, B.; Bau, R.; Thompson, M. E. *Inorg. Chem.* **2001**, *40*, 1704−1711.
(21) (a) Nazeeruddin, Md. K.; Humphry-Baker, R.; Berner, D.; Rivier, S.; Zuppiroli, L.; Graetzel, M. *J. Am. Chem. Soc.* **2003**, *125*, 8790−8797. (b) Tamayo, A. B.; Garon, S.; Sajoto, T.; Djurovich, P. I.; Tsyba, I. M.; Bau, R.; Thompson, M. E. *Inorg. Chem.* **2005**, *44*, 8723−8732.
(22) Okada, S.; Okinaka, K.; Iwawaki, H.; Furugori, M.; Hashimoto, M.; Mukaide, T.; Kamatani, J.; Igawa, S.; Tsuboyama, A.; Takiguchi, T.; Ueno, K. *Dalton Trans.* **2005**, *9*, 1583−1590.
(23) The emission spectra of **19** were measured in degassed DMSO solution at different temperatures (278 to 323 K) and shown in Figure S5 in Supporting Information, showing identical emission spectra.
(24) Mitsumori, T.; Campos, L. S.; Garcia-garibay, M. A.; Wudl, F.; Sato, H.; Sato, Y. *J. Mater. Chem.* **2009**, *19*, 5826−5836.
(25) Henwood, A. F.; Evariste, S.; Slawin, A. M. Z.; Zysman-Colman, E. *Faraday Discuss.* **2014**, *174*, 165−182.
(26) (a) Schwaebel, T.; Menning, S.; Bunz, U. H. F. *Chem. Sci.* **2014**, *5*, 1422−1428. (b) Schwaebel, T.; Trapp, O.; Bunz, U. H. F. *Chem. Sci.* **2013**, *4*, 273−281.
(27) (a) Berns, R. S.; Motta, R. J.; Gorzynski, M. E. CRT Colorimetry: Part-1 Theory and Practice, Part-2 Metrology *Color Res. Appl.*, **1993**, *18*.29910.1002/col.5080180504 (b) Brainard, D. H. *Color Res. Appl.* **1989**, *14*, 23−34. (c) http://colormine.org/convert/rgb-to-yxy.
(28) Frisch, M. J.; Trucks, G. W.; Schlegel, H. B.; Scuseria, G. E.; Robb, M. A.; Cheeseman, J. R.; Scalmani, G.; Barone, V.; Mennucci, B.; Petersson, G. A.; Nakatsuji, H.; Caricato, M.; Li, X.; Hratchian, H. P.; Izmaylov, A. F.; Bloino, J.; Zheng, G.; Sonnenberg, J. L.; Hada, M.; Ehara, M.; Toyota, K.; Fukuda, R.; Hasegawa, J.; Ishida, M.; Nakajima, T.; Honda, Y.; Kitao, O.; Nakai, H.; Vreven, T.; Montgomery, J. A., Jr.; Peralta, J. E.; Ogliaro, F.; Bearpark, M.; Heyd, J. J.; Brothers, E.; Kudin, K. N.; Staroverov, V. N.; Kobayashi, R.; Normand, J.; Raghavachari, K.; Rendell, A.; Burant, J. C.; Iyengar, S. S.; Tomasi, J.; Cossi, M.; Rega, N.; Millam, M. J.; Klene, M.; Knox, J. E.; Cross, J. B.; Bakken, V.; Adamo, C.; Jaramillo, J.; Gomperts, R.; Stratmann, R. E.; Yazyev, O.; Austin, A. J.; Cammi, R.; Pomelli, C.; Ochterski, J. W.; Martin, R. L.; Morokuma, K.; Zakrzewski, V. G.; Voth, G. A.; Salvador, P.; Dannenberg, J. J.; Dapprich, S.; Daniels, A. D.; Farkas, Ö.; Foresman, J. B.; Ortiz, J. V.; Cioslowski, J.; Fox, D. J. *Gaussian 09,* Revision D.01; Gaussian, Inc: Wallingford, CT, 2009.
(29) (a) You, Y.; Park, S. Y. *J. Am. Chem. Soc.* **2005**, *127*, 12438−12439. (b) You, Y.; Kim, K. S.; Ahn, T. K.; Kim, D.; Park, S. Y. *J. Phys. Chem. C* **2007**, *111*, 4052−4060.
(30) Dumur, F.; Lepeltier, M.; Siboni, H. Z.; Gigmes, D.; Aziz, H. *Synth. Met.* **2014**, *198*, 131−136.
(31) The mechanistic studies of dual-emissive transition metal complexes have been reported, see: (a) Blakley, R. L.; DeArmond, M. K. *J. Am. Chem. Soc.* **1987**, *109*, 4895−4901. (b) Suzuki, T.; Kuchiyama, T.; Kishi, S.; Takagi, H. D.; Kato, M. *Inorg. Chem.* **2003**, *42*, 785−795. (c) Song, L.-Q.; Feng, J.; Wang, X.-S.; Yu, J.-H.; Hou, Y.-J.; Xie, P.-H.; Zhang, B.-W.; Xiang, J.-F.; Ai, X.-C.; Zhang, J.-P. *Inorg. Chem.* **2003**, *42*, 3393−3395. (d) Glazer, E. C.; Magde, D.; Tor, Y. *J. Am. Chem. Soc.* **2005**, *127*, 4190−4192. (e) Glazer, E. C.; Magde, D.; Tor, Y. *J. Am. Chem. Soc.* **2007**, *129*, 8544−8551. (f) Sen, R.; Koner, S.; Bhattacharjee, A.; Kusz, J.; Miyashita, Y.; Okamoto, K.-I. *Dalton Trans.* **2011**, *40*, 6952−6960. Dual emission from Ir(III) complexes at 77 K temperature, see (g) King, K. A.; Watts, R. J. *J. Am. Chem. Soc.* **1987**, *109*, 1589−1590. (h) Garces, F. O.; King, K. A.; Watts, R. J. *Inorg. Chem.* **1988**, *27*, 3464−3471. (i) Wilde, A. P.; King, K. A.; Watts, R. J. *J. Phys. Chem.* **1991**, *95*, 629−634.
(32) Rouffet, M.; de Oliveira, C. A. F.; Udi, Y.; Agrawal, A.; Sagi, I.; McCammon, J. A.; Cohen, S. M. *J. Am. Chem. Soc.* **2010**, *132*, 8232−8233.
(33) *Smart & SAINT Software Reference Manuals,* Version 6.45; Bruker Analytical X-ray Systems, Inc: Madison, WI, 2003.
(34) G.M. Sheldrick, *SADABS,* Software for Empirical Absorption Correction, Ver.2.05; University of Göttingen: Germany, 2002.
(35) *XPREP,* 5.1 ed.; Siemens Industrial Automation Inc: Madison, WI, 1995.
(36) G.M. Sheldrick, *SHELXL97,* Program for Crystal Structure Refinement; University of Göttingen: Germany, 2008.

DOI: 10.1021/acs.inorgchem.5b02872
Inorg. Chem. XXXX, XXX, XXX−XXX